Article

Gut Microbiota Elicits a Protective Immune Response against Malaria Transmission

Bahtiyar Yilmaz,[1] Silvia Portugal,[2] Tuan M. Tran,[2] Raffaella Gozzelino,[1] Susana Ramos,[1] Joana Gomes,[1,3] Ana Regalado,[1] Peter J. Cowan,[4,5] Anthony J.F. d'Apice,[4,5] Anita S. Chong,[6] Ogobara K. Doumbo,[7] Boubacar Traore,[7] Peter D. Crompton,[2] Henrique Silveira,[3] and Miguel P. Soares[1,*]

[1]Instituto Gulbenkian de Ciência, Rua da Quinta Grande, 6, 2780-156 Oeiras, Portugal
[2]Laboratory of Immunogenetics, National Institute of Allergy and Infectious Diseases, National Institutes of Health, Twinbrook II, Room 125, 12441 Parklawn Drive, Rockville, MD 20852-8180, USA
[3]Centro de Malaria e Outras Doenças Tropicais, Instituto de Higiene e Medicina Tropical, Universidade Nova de Lisboa, Rua da Junqueira, 100, 1349-008 Lisboa, Portugal
[4]Immunology Research Centre, St. Vincent's Hospital, Fitzroy, Melbourne, VIC 3065, Australia
[5]Department of Medicine, University of Melbourne, Parkville, VIC 2900, Australia
[6]Section of Transplantation, Department of Surgery, University of Chicago, 5841 South Maryland Avenue, Chicago, IL 60637, USA
[7]Mali International Center of Excellence in Research, University of Sciences, Techniques and Technologies of Bamako, 1805 Bamako, Mali
*Correspondence: mpsoares@igc.gulbenkian.pt
http://dx.doi.org/10.1016/j.cell.2014.10.053

SUMMARY

Glycosylation processes are under high natural selection pressure, presumably because these can modulate resistance to infection. Here, we asked whether inactivation of the UDP-galactose:β-galactoside-α1-3-galactosyltransferase ($\alpha 1,3GT$) gene, which ablated the expression of the $Gal\alpha 1-3Gal\beta 1-4GlcNAc-R$ (α-gal) glycan and allowed for the production of anti-α-gal antibodies (Abs) in humans, confers protection against *Plasmodium spp.* infection, the causative agent of malaria and a major driving force in human evolution. We demonstrate that both *Plasmodium spp.* and the human gut pathobiont *E. coli* O86:B7 express α-gal and that anti-α-gal Abs are associated with protection against malaria transmission in humans as well as in $\alpha 1,3GT$-deficient mice, which produce protective anti-α-gal Abs when colonized by *E. coli* O86:B7. Anti-α-gal Abs target *Plasmodium* sporozoites for complement-mediated cytotoxicity in the skin, immediately after inoculation by *Anopheles* mosquitoes. Vaccination against α-gal confers sterile protection against malaria in mice, suggesting that a similar approach may reduce malaria transmission in humans.

INTRODUCTION

Humans have relatively high levels of circulating antibodies (Abs) recognizing xeno-glycans expressed by pathogens (Oyelaran et al., 2009). As for other antigens, xeno-glycans cannot be targeted by the immune system when also expressed as self-glycans. This limitation can be bypassed by natural selection of mutations that inactivate the expression of self-glycans (Bishop and Gagneux, 2007). Presumably, natural selection of such loss-of-function mutations tailored the human anti-glycan immune repertoire through evolution (Bishop and Gagneux, 2007). This notion is supported by the inactivation of the cytidine monophosphate-N-acetylneuraminic acid hydroxylase-like (*CMAH*) gene in humans, which suppressed the expression of N-glycolylneuraminic acid (Neu5Gc) (Hayakawa et al., 2001) and allowed for immune reactivity against Neu5Gc (Tangvoranuntakul et al., 2003). In a similar manner, inactivation of the $\alpha 1,3GT$ gene, which suppressed the expression of the $Gal\alpha 1-3Gal\beta 1-4GlcNAc-R$ (α-gal) carbohydrate in ancestral anthropoid primates that gave rise to humans (Galili and Swanson, 1991), also allowed for immune reactivity against α-gal (Galili et al., 1984). While it has been argued that this evolutionary process is driven to a large extent by the acquisition of immune-resistance against pathogens expressing such glycans (Bishop and Gagneux, 2007; Cywes-Bentley et al., 2013), this was never tested experimentally.

Humans do not express α-gal and up to 1%–5% of the repertoire of circulating immunoglobulin M (IgM) and immunoglobulin G (IgG) in healthy adults is directed against this glycan (Macher and Galili, 2008). Production of α-gal-specific Abs is thought to be driven by exposure to bacterial components of the microbiota expressing α-gal (Macher and Galili, 2008), including specific members of the *Klebsiella spp.*, *Serratia spp.*, and *Escherichia coli spp.* (Galili et al., 1988). Expression of α-gal by these *Enterobacteriaceae* is associated with the bacterial capsule and cell wall glycoproteins, as well as with lipopolysaccharide (LPS) (Galili et al., 1988). Gut colonization by the human pathobiont *E. coli* O86:B7 (Pal et al., 1969) recapitulates the etiology of anti-α-gal Ab production in mice (Posekany et al., 2002) and in primates (Mañez et al., 2001), as well as the production of Abs directed against the α-gal-related anti-B blood group glycan in chickens

Green: Actin/GFP **Blue**: Nuclei **Red**: α-gal
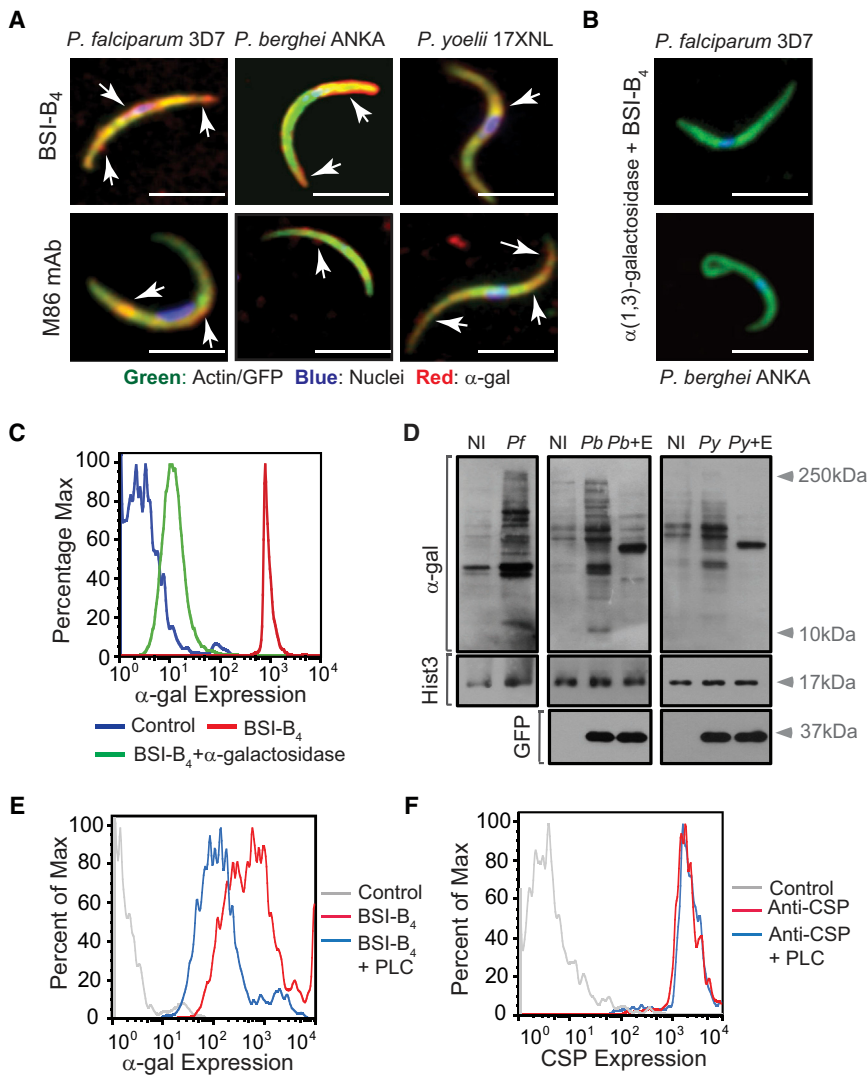
Figure 1. Detection of α-Gal in *Plasmodium* Sporozoites

(A) Composite images of GFP/actin (green), α-gal (red; white arrows), and DNA (blue) in *Plasmodium* sporozoites.

(B) Same staining as (A), after removal of α-gal by α-galactosidase. Images are representative of 2–3 independent experiments. Scale bar, 5 μm.

(C) Detection of α-gal in $PbA^{Hsp70-GFP}$ sporozoites by flow cytometry, representative of three independent experiments.

(D) Detection of α-gal in proteins extracted from salivary glands of noninfected (NI), *P. falciparum* 3D7 (*Pf*), $PbA^{Hsp70-GFP}$ (*Pb*), or *P. yoelii* 17XNL (*Py*)-infected *A.* mosquitoes. Histone H3 (Hist3) and GFP were detected as loading controls. When indicated, α-gal was digested using α-galactosidase (E).

(E and F) Detection of α-gal (E) and CSP (F) in $PbA^{Hsp70-GFP}$ sporozoites treated or not with phospholipase C (+PLC). Control is not stained. Data representative of 2–4 independent experiments.

See also Figure S1.

Malaria is transmitted to humans by the inoculation of *Plasmodium* sporozoites via the bite of female *Anopheles* (*A.*) mosquitoes (Ménard et al., 2013). While transmission may be rather efficient, only a fraction of the inoculated parasites manage to progress toward the establishment of infection (Rickman et al., 1990; Sauerwein et al., 2011; Verhage et al., 2005), hinting at a natural mechanism of protection that presumably targets the initial phases of the *Plasmodium* life cycle. Here, we demonstrate that production of anti-α-gal Abs in response to the gut *E. coli* O86:B7 pathobiont contributes critically to this natural defense mechanism, reducing malaria transmission by *A.* mosquitoes.

RESULTS

Plasmodium spp. Express the α-Gal Glycan

The α-Gal glycan was detected on the surface of *Plasmodium* sporozoites, as assessed by immunofluorescence for the human pathogen *Plasmodium falciparum* 3D7, as well as for the transgenic GFP-expressing strains of the rodent pathogens *Plasmodium berghei* ANKA (*Pb*A) or *Plasmodium yoelii* 17XNL, using the lectin *Bandeiraea* (*Griffonia*) *simplicifolia*-I isolectin IB₄ (BSI-B₄) (Galili et al., 1985) or an anti-α-gal monoclonal antibody (M86 mAb) (Galili et al., 1998) (Figure 1A; Figures S1A and S1B available online). Specificity of α-gal detection was confirmed by its enzymatic removal using α-galactosidase (Figures 1B and 1C). Expression of α-gal was associated with proteins, as assessed by western blot in whole-cell extracts from *P. falciparum* 3D7, *Pb*A, or *P. yoelii* 17XNL sporozoites

(Springer et al., 1959) and humans (Springer and Horton, 1969). This argues that gut colonization by *E. coli* O86:B7 may be particularly relevant in triggering the production of α-gal-specific Abs, presumably contributing to the high titers of these circulating Abs in healthy adult humans (Galili et al., 1988). Moreover, anti-α-gal Abs may also be produced in response to infection by pathogens expressing α-gal, such illustrated for gram-negative bacteria from *Salmonella spp.* or for protozoan parasites from *Trypanosoma spp.* (Avila et al., 1989).

Anti-α-gal Abs are cytotoxic toward α-gal-expressing pathogens, as demonstrated in vitro for bacteria (Galili et al., 1988), protozoan parasites (Avila et al., 1989), and viruses enveloped by xenogeneic α-gal-expressing cell membranes (Takeuchi et al., 1996). Whether anti-α-gal Abs confer resistance to these and/or other pathogens in vivo has, to the best of our knowledge, not been established. Here, we tested this hypothesis specifically for *Plasmodium spp.* infection, the causative agent of malaria and a major driving force that shaped the evolution of anthropoid primates, including humans.
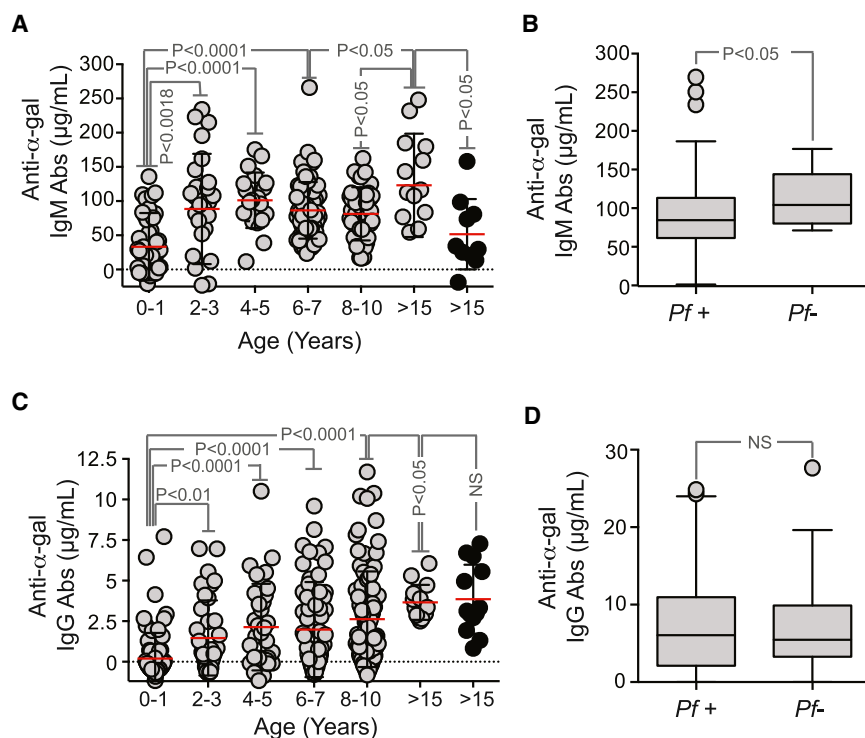
Figure 2. Anti-α-Gal IgM Abs Are Associated with Protection against Malaria Transmission in Individuals from a Malaria Endemic Region

(A) Anti-α-gal IgM Abs in individuals from a malaria endemic region in Mali (gray dots) or from the United States (black dots). Mean (red bars) ± SD.

(B) Levels of anti-α-gal IgM Abs in *P. falciparum*-infected (*Pf*+) versus noninfected (*Pf*−) children >4 years of age are shown as box plots in the same population as in (A).

(C) Anti-α-gal IgG Abs in individuals from a malaria endemic region in Mali (gray dots) or from the United States (black dots). Mean (red bars) ± SD.

(D) Levels of anti-α-gal IgG Abs in *P. falciparum*-infected (*Pf*+) versus noninfected (*Pf*−) children >4 years of age are shown as box plots in the same population as in (C).

(Figure 1D) and confirmed by enzymatic removal of α-gal (Figure 1D). Residual levels of α-gal were detected in the salivary glands of noninfected mosquitoes, suggesting that this glycan may be generated, at least partially, by *A.* mosquitoes (Figure 1D).

Expression of α-gal by *Pb*A sporozoites was reduced by ∼4-fold when the glycosylphosphatidylinositol (GPI) anchor was cleaved by phospholipase C (PLC), as assessed by flow cytometry (Figure 1E). In contrast, GPI cleavage failed to reduce the expression of circumsporozoite protein (CSP), the main protein expressed at the surface of *Plasmodium* sporozoites (Figure 1F). This suggests that α-gal is bound to GPI-anchored surface proteins, including or not CSP, which despite being GPI-anchored (Moran and Caras, 1994) is resistant to PLC cleavage (Kimmel et al., 2003) (Figure 1F).

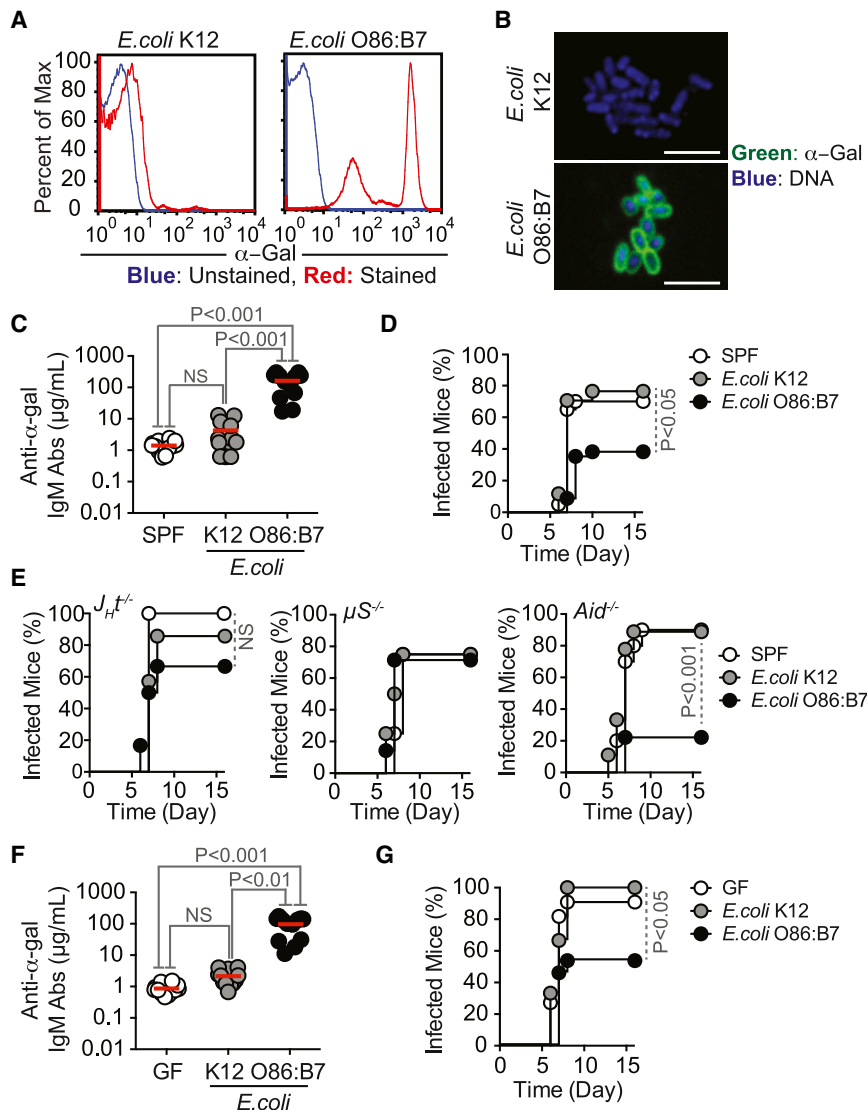### α-Gal-Specific IgM Abs Are Associated with Protection from *P. falciparum* Infection in Humans

We investigated whether a correlation exists between the levels of anti-α-gal Abs in healthy uninfected children and adults before the malaria season (n = 330 for IgG; n = 229 for IgM) and subsequent risk of *P. falciparum* infection (determined by biweekly PCR analysis of fingerprick blood samples) and febrile malaria (determined by weekly physical examination), during the ensuing 6 month malaria season in a cohort study in Mali, where this season is predictable and intense (Tran et al., 2014). In children <2 years, the average level of anti-α-gal IgM Abs was 33.4 μg/ml (95% confidence interval [CI]: 18.4–48.3 μg/ml) (Figure 2A), similar to that reported in children with no history of malaria exposure (Avila et al., 1992; Doenz et al., 2000; Galili et al., 1984; Parker et al., 1999). However, anti-α-gal IgM Abs

increased with age, reaching an average of 123.03 μg/ml (95% CI: 79.3–166.7 μg/ml) in adults— more than twice the level reported in adults with no malaria exposure, i.e., 51.6 μg/ml (95% CI: 14.9–88.3 μg/ml) (Figure 2A) (Avila et al., 1992; Doenz et al., 2000; Galili et al., 1984; Parker et al., 1999). The average level of anti-α-gal IgM Abs in children >4 years of age who had no *P. falciparum* infections detected during the 6-month malaria season (n = 13) was higher than those who became infected (n = 141) (Figure 2B). This suggests that there is a positive correlation between the levels of anti-α-gal IgM Abs and incidence of *P. falciparum* infection.

The average level of anti-α-gal IgG Abs in children <2 years was 1.46 μg/ml (95% CI: 0.22–0.69 μg/ml) and increased in adults to 3.66 μg/ml (95% CI: 3.04–4.28 μg/ml) (Figure 2C). In contrast to IgM, the levels of circulating α-gal-specific IgG were similar between malaria-exposed and nonexposed adults, suggesting that *P. falciparum* infection fails to drive an IgG response directed against α-gal (Figure 2D). This also suggests that there is no correlation between anti-α-gal IgG Abs and incidence of *P. falciparum* infection. Time-to-event analysis did not show a correlation between α-gal-specific IgM and IgG levels before the malaria season and subsequent risk of *P. falciparum* infection (p = 0.76 and p = 0.08, respectively) or febrile malaria (p = 0.35 and p = 0.18, respectively).

Gut Colonization by *E. coli* O86:B7 Elicits a Protective α-Gal-Specific IgM Ab Response against Malaria Transmission

To test whether anti-α-gal IgM Abs are protective against malaria transmission, we took advantage of "human-like" α1,3Gt-deficient mice. Unlike humans, wild-type mice have a functional α1,3Gt gene and express α-gal on secreted and cell-surface glycoconjugates, suppressing the development of anti-α-gal immunity (Yang et al., 1998). Deletion of α1,3Gt gene eliminates α-gal (Tearle et al., 1996), allowing for anti-α-gal Ab production in α1,3Gt−/− mice (Chiang et al., 2000; Tearle et al., 1996; Yang

Figure 3. Gut Colonization by *E. coli* Expressing α-Gal Protects against *Plasmodium* Infection

(A and B) Detection of α-gal in *E. coli* strains by (A) flow cytometry and (B) immunofluorescence. Representative of 2–3 independent experiments. Composite images in (B), i.e., α-gal (green) and DNA (blue) at 100× magnification. Scale bar, 10 μm.

(C and D) *α1,3Gt$^{-/-}$* mice maintained under SPF were treated with streptomycin for 7 days. (C) Anti-α-gal IgM Abs levels were measured in *α1,3Gt$^{-/-}$* mice not colonized (SPF), colonized with *E. coli* K12, or colonized with O86.B7 strains (2–3 experiments; n = 12). (D) Incidence of blood stage of *Plasmodium* infection (%) in mice colonized as in (C) and exposed to *Pb*A$^{EEF1a-GFP}$-infected *A. stephensi* mosquitoes (four experiments; n = 17–34).

(E) Incidence of blood stage of *Plasmodium* infection (%) in *α1,3Gt$^{-/-}$J_HT$^{-/-}$*, *α1,3Gt$^{-/-}$Aid$^{-/-}$*, and *α1,3Gt$^{-/-}$μS$^{-/-}$* mice colonized as in (C) and exposed to *Pb*A$^{Hsp70-GFP}$-infected *A. stephensi* mosquitoes (1–2 experiments; n = 4–10).

(F) Anti-α-gal IgM Abs were measured in GF *α1,3Gt$^{-/-}$* mice not colonized (GF), colonized with *E. coli* K12, or colonized with O86.B7 strains (2–3 experiments; n = 12). (G) Incidence of blood stage of *Plasmodium* infection (%) in mice colonized as in (F) and exposed to *Pb*A$^{EEF1a-GFP}$-infected *A. stephensi* mosquitoes (four experiments; n = 9–13).
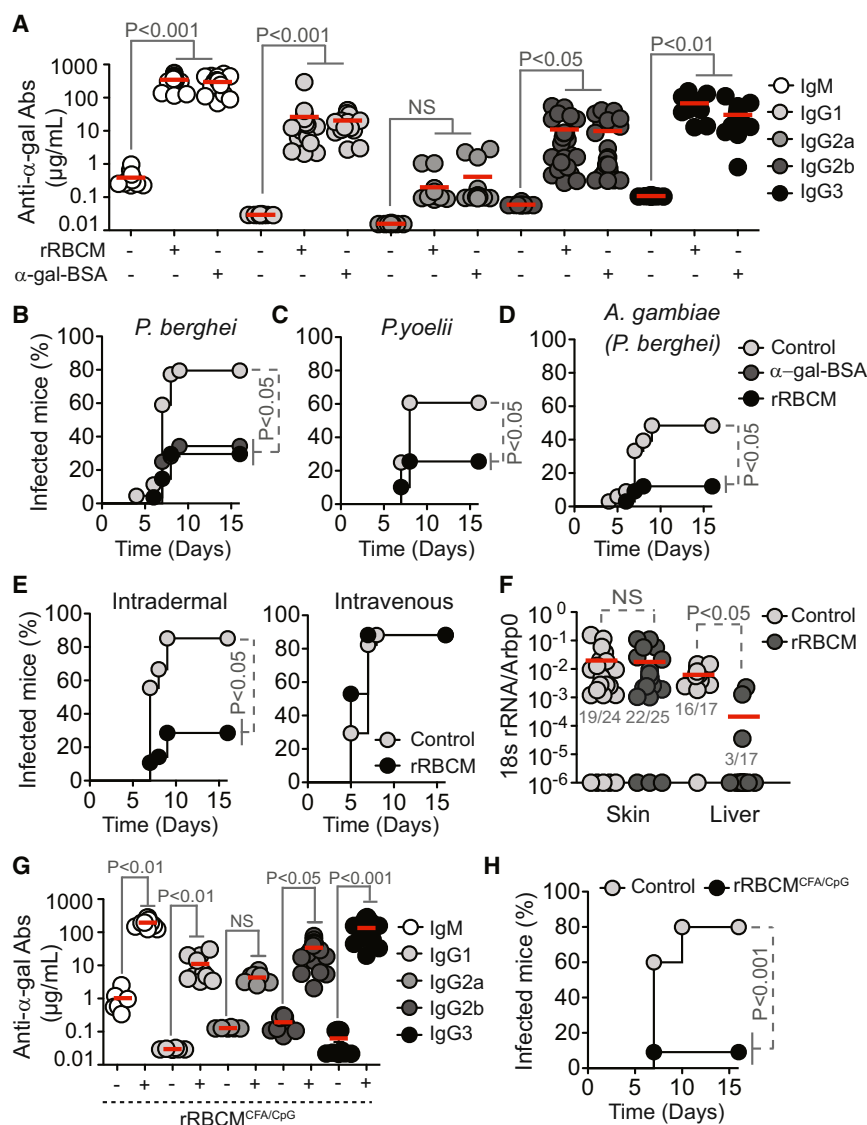
Mean (red bars).

See also Figure S2.

et al., 1998). However, *α1,3Gt$^{-/-}$* mice are known to produce only residual levels of circulating anti-α-gal Abs when maintained under specific pathogen-free (SPF) conditions (Chiang et al., 2000). Production of anti-α-gal Abs can be enhanced upon enteric exposure to *E. coli* O86:B7 (Posekany et al., 2002). We confirmed that *E. coli* O86:B7 expresses high levels of α-gal (Yi et al., 2006), which is not the case for the *E. coli* K12 strain (Figures 3A and 3B). Colonization of *α1,3Gt$^{-/-}$* mice by *E. coli* O86:B7 after antibiotic treatment (streptomycin sulfate; 5 g/l in drinking water for 7 days prior to colonization) increased the levels of circulating anti-α-gal IgM Abs from 1.4 μg/ml (95% CI: 1.1–1.8 μg/ml) to 162.9 μg/ml (95% CI: 95.89–230.1 μg/ml) before and after colonization, respectively (Figure 3C). Levels of anti-α-gal IgM Abs in colonized *α1,3Gt$^{-/-}$* mice were in the range of adult individuals from a malaria endemic region (Figure 2A). In contrast, the levels of circulating anti-α-gal IgG Abs remained at residual levels, i.e., <1 μg/ml (Figure S2A), again in the range of adult individuals from a malaria endemic region (Fig-

ure 2C). Colonization by *E. coli* K12 did not induce the production of circulating anti-α-gal Abs (Figure 3C). Gut colonization by *E. coli* O86.B7 was associated with protection of *α1,3Gt$^{-/-}$* mice from *Pb*A transmission by infected *Anopheles stephensi* mosquitoes (Figure 3D). This was not the case when *α1,3Gt$^{-/-}$* mice were or were not colonized by *E. coli* K12 (Figure 3D).

To determine whether the protective effect associated with gut colonization by *E. coli* O86.B7 is mediated by anti-α-gal Abs, we performed similar colonization experiments in *α1,3Gt$^{-/-}$J_HT$^{-/-}$* lacking B cells (Gu et al., 1993), *α1,3Gt$^{-/-}$μS$^{-/-}$* mice lacking circulating IgM (Ehrenstein et al., 1998) or *α1,3Gt$^{-/-}$Aid$^{-/-}$* mice that fail to undergo Ig class switch recombination or somatic hypermutation (Muramatsu et al., 2000). Gut colonization by *E. coli* O86.B7 failed to protect *α1,3Gt$^{-/-}$J_HT$^{-/-}$* and *α1,3Gt$^{-/-}$μS$^{-/-}$*, but not *α1,3Gt$^{-/-}$Aid$^{-/-}$* mice from *Pb*A-infected mosquitoes, as compared to genetic-matched control mice colonized or not by *E. coli* K12 (Figure 3E). This shows that the protective effect of gut colonization by *E. coli* O86.B7 acts via a mechanism mediated by anti-α-gal IgM Abs that do not undergo somatic hypermutation.

Germ-free (GF) *α1,3Gt$^{-/-}$* mice had low but detectable levels of anti-α-gal IgM Abs, i.e., 0.87 μg/ml (95% CI: 0.66–1.1 μg/ml),

Figure 4. Protective Effect of α-Gal Immunization

(A) Anti-α-gal Abs in the serum of control (−) versus rRBCM (+) or α-gal-BSA (+) immunized $\alpha1,3Gt^{-/-}$ mice (2–3 experiments; n = 12–29).

(B–D) Incidence of blood stage of infection (%) in $\alpha1,3Gt^{-/-}$ mice treated as in (A) and exposed to (B) $PbA^{EEF1a-GFP}$-infected *A. stephensi* mosquitoes (seven experiments; n = 27–44), (C) *P. yoelii* 17XNL-infected *A. stephensi* mosquitoes (five experiments; n = 28–39), or (D) $PbA^{EEF1a-GFP}$-infected *A. gambiae* mosquitoes (four experiments; n = 27–34).

(E) Incidence of blood stage of infection (%) in nonimmunized (control) versus immunized (rRBCM) $\alpha1,3Gt^{-/-}$ mice receiving $PbA^{EEF1a-GFP}$ sporozoites (3–4 experiments; n = 17–28).

(F) *Plasmodium* 18 s rRNA/*Arbp0* mRNA in skin and liver of nonimmunized (control) versus immunized (rRBCM) $\alpha1,3Gt^{-/-}$ mice exposed to $PbA^{EEF1a-GFP}$-infected *A. stephensi* mosquitoes (3–5 experiments). Infected/total mice (gray nbrs).

(G) Same as (A) in control (−) versus immunized (+; rRBCM emulsified in CFA+CpG) $\alpha1,3Gt^{-/-}$ mice (two experiments; n = 6–23).

(H) Incidence of blood stage of infection (%) in $\alpha1,3Gt^{-/-}$ mice treated as in (G) and infected as in (B) (three experiments; n = 16–19). In (A), (F), and (G), dots are individual mice and mean (red bars). See also Figures S3 and S4.

duces protection against *Plasmodium* infection, such as observed in a malaria endemic region (Figure 2).

It should be noted that the percentage of infected red blood cell (RBC), i.e., parasitemia, and incidence of mortality were similar among those $\alpha1,3Gt^{-/-}$ mice that were infected by *Pb*A regardless of colonization (Figures S2B and S2D). This suggests that gut colonization by *E. coli* O86:B7 protects against *Plasmodium* transmission, but not against disease once the erythrocytic stage of infection is established.

Immunization against α-Gal Protects from *Plasmodium* Transmission

Immunization of $\alpha1,3Gt^{-/-}$ mice against α-gal, using rabbit RBC membranes (rRBCM) expressing high levels of α-gal or synthetic α-gal conjugated to BSA (α-gal-BSA) elicited the production of circulating anti-α-gal IgM and IgG Abs (Figure 4A). Control $\alpha1,3Gt^{+/+}$ mice failed to produce anti-α-gal Abs (Chiang et al., 2000; Tearle et al., 1996; Yang et al., 1998) (Figure S3A). Circulating anti-α-gal immunoglobulin A (IgA) and immunoglobulin E (IgE) Abs were undetectable in control or immunized $\alpha1,3Gt^{-/-}$ and $\alpha1,3Gt^{+/+}$ mice (data not shown). The concentration of anti-α-gal IgM Abs in the plasma of immunized $\alpha1,3Gt^{-/-}$ mice was in the range of adult individuals from malaria endemic regions (Figure 2A). Circulating anti-α-gal IgG Abs in immunized

suggesting that these are natural Abs (Figure 3F). The production of anti-α-gal IgM Abs in GF $\alpha1,3Gt^{-/-}$ mice being driven by expression of these glycans in food components is possible, but this has not been tested. GF $\alpha1,3Gt^{-/-}$ mice did not produce anti-α-gal IgG Abs (Figure S2C). Susceptibility to *Pb*A transmission by infected *A.* mosquitoes was similar in SPF versus GF $\alpha1,3Gt^{-/-}$ mice (Figures 3D and 3G). When GF $\alpha1,3Gt^{-/-}$ mice were monocolonized by *E. coli* O86:B7, the levels of circulating anti-α-gal IgM Abs increased to 96.62 μg/ml (95% CI: 59.32–133.9 μg/ml) (Figure 3F), which is the range in which adult individuals from a malaria endemic region (Figure 2A), without concomitant induction of anti-α-gal IgG Abs (Figure S2C). Monocolonization by *E. coli* O86:B7, but not by *E. coli* K12, protected $\alpha1,3Gt^{-/-}$ mice from *Pb*A transmission by *A.* mosquitoes (Figure 3F). This suggests that gut colonization by a specific pathobiont expressing α-gal recapitulates to a large extent the normal etiology of the human anti-α-gal Ab response (Figure 2) and in-

$\alpha 1,3Gt^{-/-}$ mice, predominantly from IgG1, IgG2b, and IgG3 subclasses, were present at higher concentrations, as compared to total IgG in adult individuals from malaria endemic regions. Little or no circulating IgG2a (Figure 4A) or IgG2c (data not shown) were detected in immunized $\alpha 1,3Gt^{-/-}$ mice.

Immunization against α-gal protected $\alpha 1,3Gt^{-/-}$ mice from PbA (Figure 4B) and $P.$ $yoelli$ 17XNL (Figure 4C) transmission by infected $A.$ $stephensi$ mosquitoes, as well as from PbA transmission by $A.$ $gambiae$ mosquitoes (Figure 4D) versus control nonimmunized $\alpha 1,3Gt^{-/-}$ mice. Control immunized $\alpha 1,3Gt^{+/+}$ mice were neither protected from PbA (Figure S3B) nor $P.$ $yoelli$ 17XNL (Figure S3C) transmission by $A.$ $stephensi$ mosquitoes nor against PbA transmission by $A.$ $gambiae$ mosquitoes (Figure S3D) versus naive $\alpha 1,3Gt^{+/+}$ mice.

Immunized $\alpha 1,3Gt^{-/-}$ mice were protected from artificial transmission of PbA sporozoites via intradermal inoculation versus control nonimmunized $\alpha 1,3Gt^{-/-}$ mice (Figure 4E) or control immunized or nonimmunized $\alpha 1,3Gt^{+/+}$ mice (Figure S3E). Protection was no longer observed when sporozoites were inoculated intravenously (Figures 4E and S3E). This suggests that the protective effect of α-gal immunization is exerted in the dermis, presumably via an anti-α-gal Ab driven mechanism that is no longer effective once sporozoites reach the blood.

PbA transmission was associated with accumulation of $Plasmodium$ 18S rRNA at the site of inoculation, as quantified in the ear pinna by qRT-PCR (Figure 4F). The relative amount of $Plasmodium$ 18S rRNA was similar in immunized versus control nonimmunized $\alpha 1,3Gt^{-/-}$ mice (Figure 4F) or control immunized or nonimmunized $\alpha 1,3Gt^{+/+}$ mice (Figure S3F). Immunized $\alpha 1,3Gt^{-/-}$ mice did not accumulate $Plasmodium$ 18S rRNA in the liver, when compared to control nonimmunized $\alpha 1,3Gt^{-/-}$ mice (Figure 4F) or control nonimmunized or immunized $\alpha 1,3Gt^{+/+}$ mice (Figure S3F). This suggests that α-gal immunization arrests the transit of inoculated sporozoites from the skin into the liver, without interfering with sporozoite inoculation by $A.$ mosquitoes.

TLR9 Agonist Adjuvant Enhances the Protective Effect of α-Gal Immunization

Immunization of $\alpha 1,3Gt^{-/-}$ mice with rRBCM emulsified in complete Freund's adjuvant (CFA), supplemented with toll-like receptor 9 agonist CpG, enhanced anti-α-gal IgG2b and IgG3 Ab response by 2- to 3-fold (Figure 4G) versus immunization without adjuvant (Figure 4A). This was associated with 88% reduction in the relative risk of transmission of PbA infection by $A.$ mosquitoes (95% CI: 0.032–0.452) versus 61% reduction upon immunization without adjuvant (95% CI: 0.209–0.726) (Figures 4B and 4H). This protective effect was not observed in control $\alpha 1,3Gt^{+/+}$ mice (Figures S3G and S3H).

Parasitemias were similar in immunized $\alpha 1,3Gt^{-/-}$ mice not protected from PbA infection versus control nonimmunized $\alpha 1,3Gt^{-/-}$ mice as well as control nonimmunized or immunized $\alpha 1,3Gt^{+/+}$ mice (data not shown). Moreover, when infected, all mice succumbed to experimental cerebral malaria. This suggests that while protective against malaria transmission, α-gal immunization is not protective against the development of severe disease if $Plasmodium$ manages to establish infection. In keeping with this notion, when inoculated with PbA-infected RBC, immunized $\alpha 1,3Gt^{-/-}$ mice developed similar levels of parasitemia and disease severity, as compared to control nonimmunized $\alpha 1,3Gt^{-/-}$ mice as well as to control nonimmunized or immunized $\alpha 1,3Gt^{+/+}$ mice (Figure S4A).

We tested further whether the protective effect conferred by α-gal immunization is associated with sterile protection, i.e., inability of $Plasmodium$ to establish blood stage of infection. Passive transfer of RBCs harvested from protected immunized $\alpha 1,3Gt^{-/-}$ mice at day 8–9 post-PbA transmission by $A.$ mosquitoes failed to transmit disease to naive $\alpha 1,3Gt^{-/-}$ mice (Figure S4B). In contrast, passive transfer of RBC harvested from nonprotected immunized $\alpha 1,3Gt^{-/-}$ mice, readily transmitted disease to naive $\alpha 1,3Gt^{-/-}$ mice (Figure S4B). This demonstrates that the protective effect of immunization against α-gal is associated with sterile protection against malaria.

Anti-α-Gal IgM and IgG Abs Produced in Response to α-Gal Immunization Confer Protection against Malaria Transmission

We asked whether the protective effect of α-gal immunization is mediated by anti-α-gal IgM and/or IgG Abs. Immunized $\alpha 1,3Gt^{-/-}J_HT^{-/-}$ mice failed to produce anti-α-gal IgM or IgG Abs versus naive $\alpha 1,3Gt^{-/-}J_HT^{-/-}$ mice or immunized $\alpha 1,3Gt^{-/-}$ mice (Figure 5A). Moreover, immunized $\alpha 1,3Gt^{-/-}J_HT^{-/-}$ mice were not protected against PbA transmission by $A.$ mosquitoes versus control nonimmunized $\alpha 1,3Gt^{-/-}J_HT^{-/-}$ mice (Figure 5B). This shows that the protective effect of α-gal immunization is mediated via a B cell-dependent mechanism.

Immunization of $\alpha 1,3Gt^{-/-}Aid^{-/-}$ mice failed to induce the production of anti-α-gal IgG, but not IgM Abs, versus naive $\alpha 1,3Gt^{-/-}Aid^{-/-}$ or immunized $\alpha 1,3Gt^{-/-}$ mice (Figure 5A). Immunized $\alpha 1,3Gt^{-/-}Aid^{-/-}$ mice were nevertheless protected against PbA transmission by $A.$ mosquitoes versus nonimmunized $\alpha 1,3Gt^{-/-}Aid^{-/-}$ mice (Figure 5B). This confirms that anti-α-gal IgM Abs can confer protection against malaria transmission (Figure 2B) and that the protective effect of α-gal-specific IgM Abs does not require somatic hypermutation.

Immunization of $\alpha 1,3Gt^{-/-}\mu S^{-/-}$ mice failed to induce anti-α-gal IgM Abs, without interfering with anti-α-gal IgG Ab response versus naive $\alpha 1,3Gt^{-/-}\mu S^{-/-}$ mice or immunized $\alpha 1,3Gt^{-/-}$ mice (Figure 5A). Immunized $\alpha 1,3Gt^{-/-}\mu S^{-/-}$ mice were nevertheless protected from PbA transmission by $A.$ mosquitoes versus control naive $\alpha 1,3Gt^{-/-}\mu S^{-/-}$ mice (Figure 5B). Immunized $\alpha 1,3Gt^{-/-}$ mice did not produce circulating anti-α-gal IgA or IgE Abs (data not shown) and a putative protective effect for these Ig isotypes was excluded. This demonstrates that anti-α-gal IgG Abs produced in response to immunization confer protection against malaria transmission.

Immunization of $\alpha 1,3Gt^{-/-}Tcr\beta^{-/-}$ mice lacking mature $\alpha\beta$ T cells (Mombaerts et al., 1992) compromised anti-α-gal IgM and IgG response versus control immunized $\alpha 1,3Gt^{-/-}$ mice (Figure 5A). Immunized $\alpha 1,3Gt^{-/-}Tcr\beta^{-/-}$ mice were not protected from PbA transmission by $A.$ mosquitoes versus control naive $\alpha 1,3Gt^{-/-}Tcr\beta^{-/-}$ mice (Figure 5B). This shows that anti-α-gal Abs produced in response to immunization are T cell-dependent (Cretin et al., 2002) and so is their protective effect.
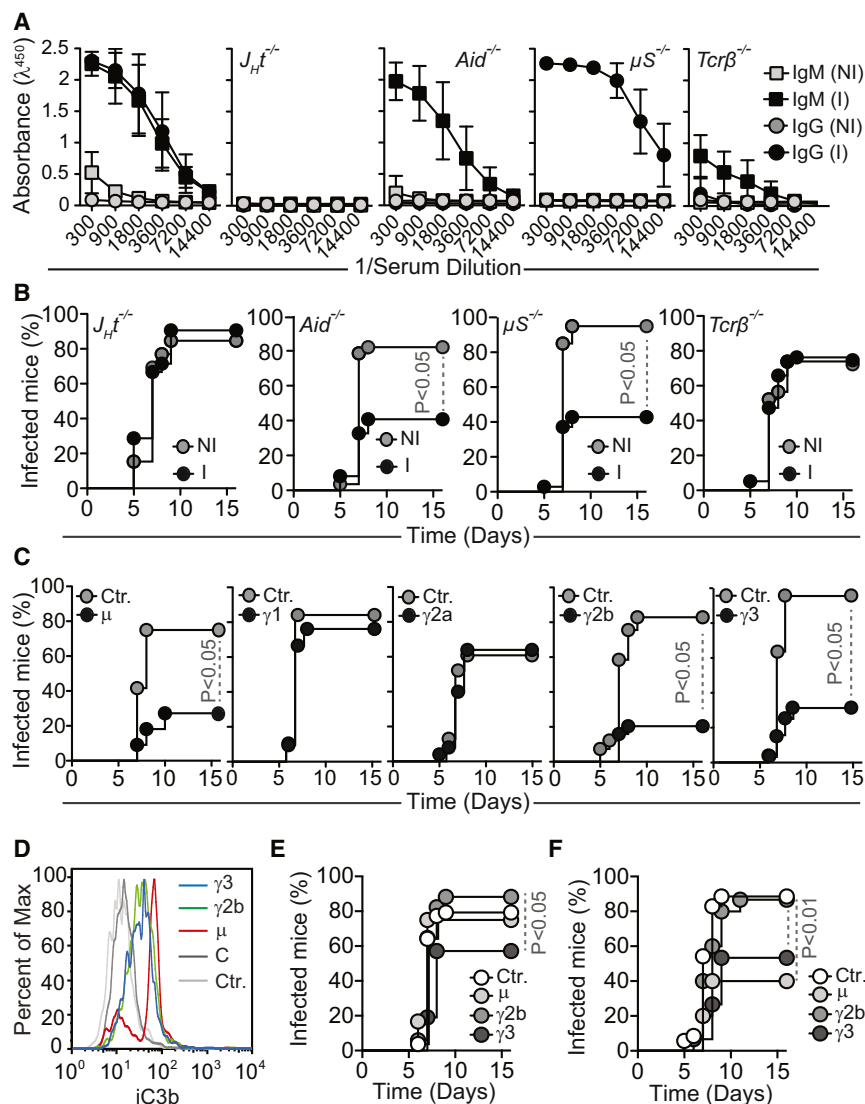
Figure 5. Protective Effect of Anti-α-Gal Abs

(A) Relative absorbance of anti-α-gal Abs (Mean ± SD) in serial serum dilutions from nonimmunized (NI) or rRBCM-immunized (I) $\alpha1,3Gt^{-/-}$ mice (two experiments; n = 10).

(B) Incidence of blood stage infection (%) in specific immune component-deleted $\alpha1,3Gt^{-/-}$ mice immunized (I) or not (NI) as in (A) and exposed to $PbA^{EEF1a-GFP}$-infected mosquitoes (3–7 experiments; n = 13–41).

(C) Incidence of blood stage of infection (%) in $\alpha1,3Gt^{-/-}$ mice after passive transfer of anti-α-gal Abs versus controls (no passive transfer; ctr.) exposed to $PbA^{EEF1a-GFP}$-infected mosquitoes (4–7 experiments; n = 19–32).

(D) C3 deposition in $PbA^{Hsp70-GFP}$ sporozoites not exposed (ctr.) or exposed to anti-α-gal Abs plus mouse complement (C). Representative of three independent experiments.

(E) Incidence of blood stage of infection (%) in $\alpha1,3Gt^{-/-}C3^{-/-}$ mice after passive transfer of anti-α-gal IgM (μ), IgG2b (γ2b), or IgG3 (γ3) Abs versus controls (ctr.; no passive transfer) not receiving Abs, exposed to $PbA^{EEF1a-GFP}$-infected mosquitoes (four experiments; n = 21–37).

(F) Same as (E) in PMN-depleted $\alpha1,3Gt^{-/-}$ mice (four experiments; n = 15–25).
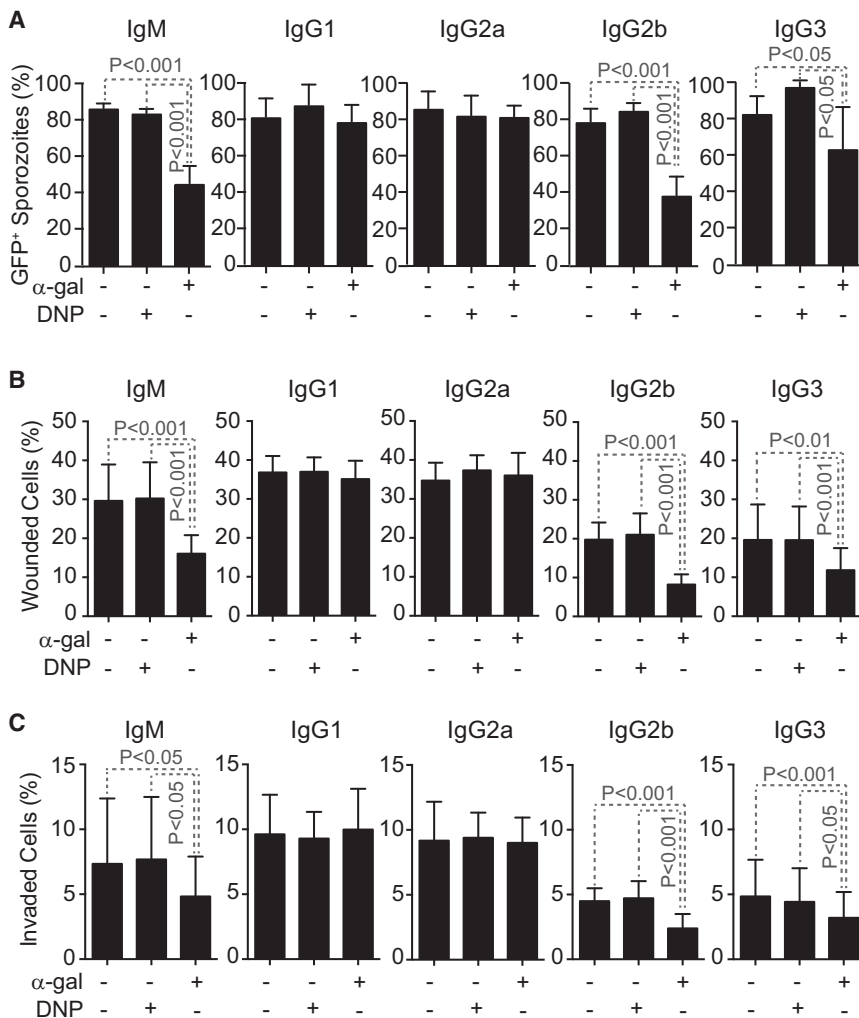
See also Figures S5 and S6.

face of *Plasmodium* sporozoites (Figure S6C). IgG2a, IgG2b, and IgG3 mAbs are class-switched mutants derived from the original anti-α-gal IgG1 clone and as such have similar affinities for α-gal (Ding et al., 2008). These data reveal that while IgM anti-α-gal Abs are sufficient per se to confer protection against malaria transmission, this protective effect can be enhanced when specific subclasses anti-α-gal IgG Abs are present at sufficient high levels.

Once bound to the surface of *Plasmodium* sporozoites, anti-α-gal IgM, IgG2b, and IgG3 mAbs activated the classical pathway of complement, as assessed by C3 deposition (Figure 5D). Anti-α-gal IgG1 or IgG2a mAbs failed to activate complement (data not shown), and complement activation was also not observed in the absence of anti-α-gal Abs (Figures 5D and S7), showing that the alternative and lectin pathways of complement are not activated by *Plasmodium* sporozoites.

We then asked whether the protective effect exerted by anti-α-gal Abs is mediated via a mechanism involving the activation of the complement cascade (Figure 5D) (Ding et al., 2008; Miyatake et al., 1998). Passive transfer of anti-α-gal IgM Abs or anti-α-gal IgG2b mAb to $\alpha1,3Gt^{-/-}C3^{-/-}$ mice, which lack C3 and cannot activate the complement cascade, failed to confer protection against PbA transmission versus control $\alpha1,3G^{-/-}C3^{-/-}$ mice (Figure 5E). Passive transfer of anti-α-gal IgG3 mAb to $\alpha1,3Gt^{-/-}C3^{-/-}$ mice conferred residual but significant protection versus control $\alpha1,3G^{-/-}C3^{-/-}$ mice (Figure 5E). This

Naive and immunized $\alpha1,3Gt^{-/-}J_HT^{-/-}$ (Figure S5A), $\alpha1,3Gt^{-/-}Aid^{-/-}$, (Figure S5B) and $\alpha1,3Gt^{-/-}\mu S^{-/-}$ (Figure S5C) mice, not protected from PbA transmission, developed similar levels of parasitemia and succumbed to experimental cerebral malaria. This was not the case for $\alpha1,3Gt^{-/-}Tcr\beta^{-/-}$ mice (Figure S5D), consistent with the involvement of T cells in the pathogenesis of experimental cerebral malaria (Belnoue et al., 2002).

Passive transfer of anti-α-gal IgM to naive $\alpha1,3Gt^{-/-}$ mice conferred protection against PbA transmission by A. mosquitoes (Figure 5C). This was also the case for passive transfer of anti-α-gal Abs from specific IgG subclasses, namely, IgG2b and IgG3 (Figure 5C), but not IgG1 or IgG2a (Figure 5C). Relative binding to α-gal was similar for all mAbs tested, as assessed by ELISA using α-gal-BSA as a solid-phase antigen (Figure S6A) or by immunofluorescence using PbA sporozoites (Figure S6B). Specificity of anti-α-gal binding to *Plasmodium* sporozoites was assessed by enzymatic removal of α-gal, confirming that these mAbs recognize specifically and only the α-gal glycan on the sur-

Figure 6. Protective Effect of Anti-α-Gal Abs against Hepatocyte Infection

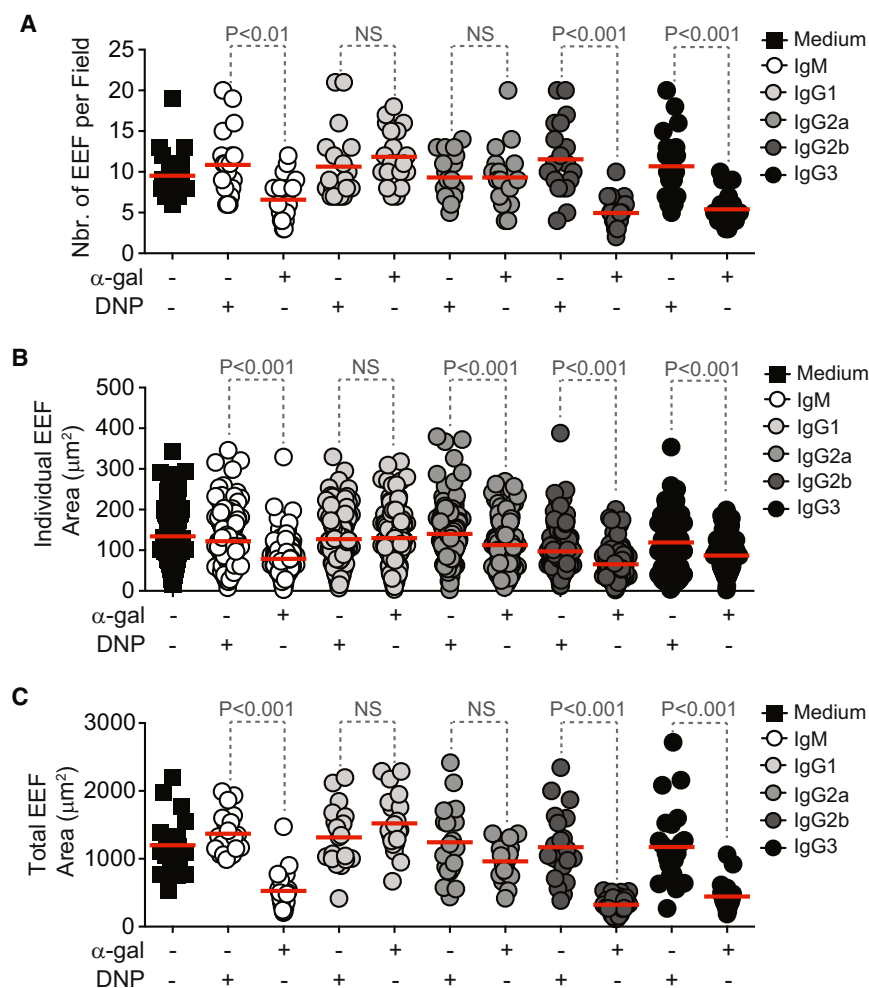(A) Mean percentage (%) of viable GFP⁺ *Pb*A^Hsp70-GFP sporozoites ± STD (3–4 experiments) after exposure in vitro to anti-α-gal or control anti-DNP mAbs in the presence of mouse complement. (B and C) Mean percentage (%) of HepG2 cells (B) wounded (Dextran-Red⁺) or (C) invaded (GFP⁺) by *Pb*A^Hsp70-GFP sporozoites treated as in (A) ± SD (six experiments).

while preventing the onset of cerebral malaria (data not shown), consistent with previous findings (Chen et al., 2000).

Anti-α-Gal Abs Are Cytotoxic to *Plasmodium* Sporozoites

Complement activation by anti-α-gal IgM, IgG2b, or IgG3 mAb was cytotoxic to *Pb*A sporozoites in vitro, as assessed by sporozoite GFP expression (Figure 6A). Anti-α-gal IgG1 and IgG2a mAbs, which did not activate complement when bound to *Plasmodium* sporozoites (data not shown), were not cytotoxic (Figure 6A). The cytotoxic effect of anti-α-gal IgM, IgG2b, and IgG3 was similar when using mouse (Figure 6A) or rabbit (Figure S7A) complement but was strictly dependent on the presence of complement (Figure S7B). A similar cytotoxic effect was observed when quantifying viable "crescent-shaped" sporozoites (Figure S7C), an independent readout for sporozoite viability (Hegge et al., 2010). Isotype-matched control anti-dinitrophenyl (DNP) Abs were not cytotoxic to *Pb*A sporozoites in vitro (Figures 6A and S7A–S7C).

Anti-α-Gal Abs Inhibit Hepatocyte Invasion by *Plasmodium* Sporozoites

We asked whether anti-α-gal Abs inhibit hepatocyte transmigration (wounding) and/or hepatocyte invasion by *Plasmodium* sporozoites (Mota et al., 2001). Complement activation by anti-α-gal IgM, IgG2b, and IgG3 Abs inhibited hepatocyte transmigration (Figure 6B) and invasion (Figure 6C), as assessed in vitro for *Pb*A sporozoites. This inhibitory effect was not observed when using anti-α-gal IgG1 or IgG2a Abs or isotype/subclass-matched control anti-DNP Abs (Figures 6B and 6C).

We then assessed whether anti-α-gal Abs inhibit the development of exoerythrocytic forms (EEF) of *Plasmodium*. Complement activation by anti-α-gal IgM, IgG2b, and IgG3 Abs reduced the number of EEF (Figure 7A), as well as the average EEF size (Figures 7B and 7C) formed in vitro by *Pb*A sporozoites. Anti-α-gal IgG1 Abs did not show this inhibitory effect, while anti-α-gal IgG2a Abs did not reduce the number of EEF (Figure 7A) but had a residual inhibitory effect on EEF size (Figures 7B and

suggests that the protective effect exerted by anti-α-gal IgM and IgG2b Abs acts via a mechanism that is strictly complement dependent, whereas the protective effect of anti-α-gal IgG3 Abs is partially but probably not strictly dependent on complement activation. Infection incidence was similar in control *α1,3Gt*⁻/⁻ *C3*⁻/⁻ versus *α1,3Gt*⁻/⁻*C3*⁺/⁺ mice (Figures 5C and 5E).

Complement activation generates C3a and C5a chemoattractants that promote IgG-dependent polymorphonuclear (PMN) cell cytotoxicity (Ding et al., 2008; Nimmerjahn and Ravetch, 2008; Yin et al., 2004). Therefore, we asked whether the protective effect of anti-α-gal Abs involves PMN cells. Passive transfer of anti-α-gal IgG2b Abs to *α1,3Gt*⁻/⁻ mice, depleted from PMN cells by the administration of anti-Ly-6G (Gr-1) (Porcherie et al., 2011), failed to confer protection against *Pb*A transmission by *A.* mosquitoes, whereas passive transfer of anti-α-gal IgM or IgG3 Abs conferred protection (Figure 5F). This suggests that the protective effect exerted by anti-α-gal IgM and IgG2b Abs acts via a mechanism strictly dependent on PMN cells, whereas the protective effect of anti-α-gal IgG3 Abs is partially but probably not strictly dependent on PMN cells. Depletion of PMN cells per se did not interfere with *Plasmodium* infection (Figure 5F)

Figure 7. Protective Effect of Anti-α-Gal Abs against *Plasmodium* Maturation in Hepatocytes

(A) Number of EEF per field (dots; 20–23 fields).

(B) Area of individual EEF (dots) (n = 111–256 EEFs counted in 20–23 fields).

(C) Total area of EEF (dots) per field (20–23 fields). HepG2 cells were incubated with *Pb*A^Hsp70-GFP sporozoites, previously exposed to anti-α-gal or control anti-DNP mAbs in the presence of complement (A–C).

See also Figure S7.

The protective effect exerted by anti-α-gal IgM Abs should be relevant to understand why malaria incidence is higher in children versus adults from malaria endemic regions (Modiano et al., 1996). Relative absence of these antibodies in children under the age of 2–3 years should favor malaria transmission, as compared to adults that have higher levels of circulating anti-α-gal IgM Abs (Figure 2A). This relative absence of anti-α-gal IgM in children may be explained by the (1) kinetics of establishment of an adult-like gut microbiota (Ringel-Kulka et al., 2013), (2) requirement of environmental and dietary exposure in the establishment of an adult-like gut microbiota, and/or (3) the kinetics of the establishment of adult-like B cell repertoire, including anti-α-gal B cells.

The protective effect exerted by anti-α-gal IgM Abs might also contribute to explain why only a small fraction of *Plasmodium* sporozoites inoculated by mosquitoes manage to progress toward the establishment of infection in humans. This is true even when *Plasmodium* sporozoites are inoculated under controlled experimental conditions in adults (Rickman et al., 1990; Sauerwein et al., 2011; Verhage et al., 2005). Presumably, when present at sufficient high levels in adults, circulating anti-α-gal IgM Abs prevent the large majority of *Plasmodium* sporozoites from establishing a successful infection. However, infection is established if as few as a couple of *Plasmodium* sporozoites manage to escape this natural mechanism of protection.

Whether α-gal detected at the surface of *Plasmodium* sporozoites (Figure 1) is produced by *Plasmodium* and/or by the mosquito is not clear. The salivary glands of noninfected mosquitoes express low levels of α-gal, as detected by western blot (Figure 1) and immunostaining (data not shown). *Plasmodium* sporozoites are masked by mosquito laminin (Warburg et al., 2007), an evolutionary conserved glycoprotein that in other species contains α-gal (Takahashi et al., 2014). It is possible therefore that anti-α-gal Abs recognize laminin or another mosquito-derived protein expressing α-gal, masking *Plasmodium* sporozoites (Warburg et al., 2007).

7C). Isotype/subclass-matched control anti-DNP Abs did not modulate EEF numbers (Figure 7A) or average size (Figures 7B and 7C).

DISCUSSION

When inoculated in humans through the bite of an *A.* mosquito, *Plasmodium* sporozoites are confronted with relatively high levels of cytotoxic anti-α-gal IgM Abs (Figure 2A). That these Abs are protective against malaria transmission is supported by three independent lines of evidence. First, individuals from a malaria endemic region that show evidence of decreased *P. falciparum* infection risk have higher levels of circulating α-gal-specific IgM Abs, as compared to individuals who are susceptible to *P. falciparum* infection (Figure 2B). Second, when present at levels similar to those observed in individuals from a malaria endemic region—in α*1,3Gt*$^{-/-}$ mice colonized by human gut pathobiont *E. coli* O86:B7 expressing α-gal (Figure 3) or in immunized α*1,3Gt*$^{-/-}$ mice (Figures 4A and 4B)—anti-α-gal IgM Abs confer protection against malaria transmission. Third, passive transfer of anti-α-gal IgM Abs is sufficient per se to protect α*1,3Gt*$^{-/-}$ mice from malaria transmission (Figure 5C).

It is now well established that specific components of the gut microbiota can modulate immunity and resistance to infection (Belkaid and Hand, 2014; Honda and Littman, 2012). In support of this notion, resistance to viral and bacterial (Fagundes et al., 2012) infections is impaired in GF mice (Dolowy and Muldoon, 1964) or mice subjected to antibiotic-driven dysbiosis (Ichinohe et al., 2011). We reasoned that xeno-glycans expressed by specific components of the gut microbiota might trigger a protective immune response against pathogens expressing the same xeno-glycans. We show that this is the case for α-gal, a xeno-glycan expressed by the human gut pathobiont *E. coli* O86:B7, as well by *Plasmodium spp.* (Figures 1, 3A, and 3B). When colonized by *E. coli* O86:B7, $\alpha 1,3Gt^{-/-}$ mice produce an anti-α-gal IgM Ab response (Figures 3C and 3F) that confer protection against *Plasmodium* infection (Figures 3D, 3E, 3G, and 5C) via a lytic mechanism mediated by complement activation (Figures 5E and 6A). It is worth noticing that in a similar manner to other microbiota-driven resistance mechanisms, the protective effect exerted by *E. coli* O86:B7 acts at the level of a tissue barrier, i.e., the skin, to prevent *Plasmodium* transmission (Figures 4E and 4F).

Levels of circulating anti-α-gal IgG Abs in individuals from a malaria endemic region (Figure 2C), as well as in $\alpha 1,3Gt^{-/-}$ mice colonized with *E. coli* O86:B7 (Figures S2A and S2C), are ~30-fold and ~40 to 70-fold, respectively, lower than levels of IgM anti-α-gal Abs. This may explain why basal levels anti-α-gal IgG Abs in individuals from a malaria endemic region are not associated with decreased risk of *P. falciparum* infection (Figure 2D). This also suggests that *P. falciparum* infection fails to induce class switch of the anti-α-gal Ig Ab response in those individuals. It is possible therefore that *P. falciparum* represses Ig class-switch recombination, explaining the residual levels of circulating anti-α-gal IgG Abs (Figure 2C).

While anti-α-gal Abs can provide sterile protection against malaria in mice (Figures 5B, 5C, and S4B), this is not commonly observed in malaria endemic regions in which adult individuals have circulating anti-α-gal IgM Abs, possibly because the levels of these Abs are below a threshold level required to provide sterile protection (Figure 2). However, we show that this natural mechanism of protection can be enhanced via immunization using adjuvants that favor the production of T cell-dependent complement fixing anti-α-gal IgG Abs (Figures 4G and 4H). Moreover, when coupled to *Plasmodium* antigens, this approach should enhance the immunogenicity of such antigens (Benatuil et al., 2005) and boost the protective efficacy of candidate malaria vaccines based on such antigens (Olotu et al., 2013). This approach should be useful in preventing not only individual infections but also disease transmission given the protective effect of anti-α-gal Abs.

It is possible that the protective effect of "attenuated" sporozoite vaccine trials against malaria (Seder et al., 2013) is driven to some extent by an anti-α-gal Ab response, given the expression of α-gal by *Plasmodium falciparum* sporozoites (Figure 1). Whether a correlation can be established between the effectiveness of such candidate vaccines and a putative anti-α-gal IgG Ab response has not been established but may be useful to consider as a retrospective analyzes.

As a final note, we predict that in a similar manner to anti-α-gal Abs other anti-glycan Abs may confer protection against malaria

as well as other vector-borne protozoan parasites (Huflejt et al., 2009; Lacroix-Desmazes et al., 1995; Nagele et al., 2013). Moreover, anti-α-gal Abs may also target other vector-borne protozoan parasites expressing α-gal, such as *Leishmania spp.* and *Trypanosoma spp.*, the causative agents of Leishmaniasis and Trypanosomiasis, respectively (Avila et al., 1989). As such, vaccination approaches similar to the one proposed here for malaria may be considered against these diseases as well.

EXPERIMENTAL PROCEDURES

Cohort Study

For detailed analysis, see the Extended Experimental Procedures.

Immunization against α-Gal

Eight- to ten-week-old mice received 3×10^8 rabbit rRBCM equivalents (100 μl; PBS; intraperitoneal [i.p.]). Adjuvants are described in the Extended Experimental Procedures. Mouse serum was collected 2 weeks after last immunization, and circulating anti-α-gal Abs were quantified by ELISA. See the Extended Experimental Procedures for details on anti-α-gal ELISA.

Passive Transfer of Anti-α-Gal mAbs

$\alpha 1,3Gt^{-/-}$ mice received anti-α-gal IgG1, IgG2a, IgG2b, and IgG3 mAbs (Ding et al., 2008; Yin et al., 2004) (150 μg; 100 μl per mouse) or polyclonal IgM (150 μg; 300–400 μl per mouse) via a single intravenous (i.v.) injection 24 hr prior to mosquito exposure.

Plasmodium Strains

Transgenic *P. berghei* ANKA (*PbA*) strains expressing GFP under the *eef1α* promoter, i.e., $PbA^{EEF1a\text{-}GFP}$ (259cl1; MR4; MRA-865) (Franke-Fayard et al., 2004), or under the *hsp70* promoter (Ishino et al., 2006), i.e., $PbA^{Hsp70\text{-}GFP}$ (kindly provided by Robert Menard, Institut Pasteur), transgenic *P. yoelii* 17XNL strain expressing GFP under the *PbA eef1α* promoter (MR4; MRA-817; kindly provided by Robert Menard, Institut Pasteur) (Weiss et al., 1989). For sporozoite production, see the Extended Experimental Procedures.

Plasmodium Transmission

A. stephensi or *gambiae* mosquitoes were allowed to feed on anesthetized mice (i.p.; 125 mg/kg ketamine; 12.5 mg/kg xylazine) placed on a warming tray. Two mosquitoes were allowed to probe and feed independently (90–100 s) on restricted to the edge of the mouse ear (10–12/3–4 mm) and dissected thereafter for confirmation of sporozoites in salivary glands. If negative, infection was repeated.

Sporozoites Inoculation

$PbA^{EEF1a\text{-}GFP}$ sporozoites were inoculated (i.d.) in the ear pinna (750 sporozoites in 20–30 μl; 1% BSA in PBS) or i.v. in the retro-orbital vein (150 sporozoites in 50 μl; 1% BSA in PBS) using a microsyringe (Nanofil 100 μl; 33G beveled needle; World Precision Instruments).

Detection of α-Gal in *Plasmodium* Sporozoites

Sporozoites were stained with Alexa Fluor 647-conjugated BSI-IB$_4$ or Alexa Fluor 647-conjugated anti-α-gal mAbs and detected by confocal microscope or flow cytometer. For detection of α-gal in $PbA^{Hsp70\text{-}GFP}$ by western blotting, see the Extended Experimental Procedures. Green coffee bean α-galactosidase (50–200 μl; 5 U/ml; 60–90 min; 25°C; Sigma Chemical) was used to hydrolyze terminal α-galactosyl moieties from glycolipids and glycoproteins (Luo et al., 1999).

Statistical Analysis

All tests (except human cohort studies) were performed using the GraphPad Prism (v. 6.0) (GraphPad Software). Human analyses were performed in R (v. 3.0.2). Detailed analyses are described in the Extended Experimental Procedures.

Mice

Experiments in mice were performed in accordance with protocols approved by the Ethics Committee of the Instituto Gulbenkian de Ciência and the Portuguese National Entity (DGAV-Direção Geral de Alimentação e Veterinária). Experiments in mice were performed in accordance with the Portuguese (Decreto-Lei no. 113/2013) and European (directive 2010/63/EU) legislation related to housing, husbandry, and animal welfare. C57BL/6 $J_HT^{-/-}$ (Gu et al., 1993), $Tcr\beta^{-/-}$ (Mombaerts et al., 1992), $Aid^{-/-}$ (Muramatsu et al., 2000), $\mu S^{-/-}$ (Ehrenstein et al., 1998), and $C3^{-/-}$ (Circolo et al., 1999) mice were crossed with C57BL/6 $\alpha1,3Gt^{-/-}$ mice (Shinkel et al., 1997; Tearle et al., 1996). For the details on genotyping, see the Extended Experimental Procedures.

SUPPLEMENTAL INFORMATION

Supplemental Information includes Extended Experimental Procedures and seven figures and can be found with this article online at http://dx.doi.org/10.1016/j.cell.2014.10.053.

AUTHOR CONTRIBUTIONS

B.Y. contributed to study design, performed, and/or contributed critically to all experiments, analyzed data, and contributed to writing of the manuscript. In some experiments, B.Y. was assisted by S.R., S.P., T.M.T., and P.D.C. designed, performed, and analyzed the human studies. R.G. performed the western blot experiments. H.S. supervised J.G. in the establishment and maintenance of *Plasmodium*-infected *A.* mosquitoes. A.R. produced and troubleshooted all mAb production. P.J.C. and A.J.F.A. generated $\alpha1,3Gt^{-/-}$ mice. A.S.C. provided anti-α-gal hybridomas. O.K.D. and B.T. organized the human studies and provided the human serum samples. M.P.S. formulated the original hypothesis, drove the study design, and wrote the manuscript with B.Y. All authors read and approved the manuscript.

REFERENCES

Avila, J.L., Rojas, M., and Galili, U. (1989). Immunogenic Gal alpha 1——3Gal carbohydrate epitopes are present on pathogenic American Trypanosoma and Leishmania. J. Immunol. *142*, 2828–2834.

Avila, J.L., Rojas, M., and Velazquez-Avila, G. (1992). Characterization of a natural human antibody with anti-galactosyl(alpha 1-2)galactose specificity that is present at high titers in chronic Trypanosoma cruzi infection. Am. J. Trop. Med. Hyg. *47*, 413–421.

Belkaid, Y., and Hand, T.W. (2014). Role of the microbiota in immunity and inflammation. Cell *157*, 121–141.

Belnoue, E., Kayibanda, M., Vigario, A.M., Deschemin, J.C., van Rooijen, N., Viguier, M., Snounou, G., and Rénia, L. (2002). On the pathogenic role of brain-sequestered alphabeta CD8+ T cells in experimental cerebral malaria. J. Immunol. *169*, 6369–6375.

Benatuil, L., Kaye, J., Rich, R.F., Fishman, J.A., Green, W.R., and Iacomini, J. (2005). The influence of natural antibody specificity on antigen immunogenicity. Eur. J. Immunol. *35*, 2638–2647.

Bishop, J.R., and Gagneux, P. (2007). Evolution of carbohydrate antigens—microbial forces shaping host glycomes? Glycobiology *17*, 23R–34R.

Chen, L., Zhang, Z., and Sendo, F. (2000). Neutrophils play a critical role in the pathogenesis of experimental cerebral malaria. Clin. Exp. Immunol. *120*, 125–133.

Chiang, T.R., Fanget, L., Gregory, R., Tang, Y., Ardiet, D.L., Gao, L., Meschter, C., Kozikowski, A.P., Buelow, R., and Vuist, W.M. (2000). Anti-gal antibodies in humans and 1, 3alpha-galactosyltransferase knock-out mice. Transplantation *69*, 2593–2600.

Cretin, N., Bracy, J., Hanson, K., and Iacomini, J. (2002). The role of T cell help in the production of antibodies specific for Gal alpha 1-3Gal. J. Immunol. *168*, 1479–1483.

Cywes-Bentley, C., Skurnik, D., Zaidi, T., Roux, D., Deoliveira, R.B., Garrett, W.S., Lu, X., O'Malley, J., Kinzel, K., Zaidi, T., et al. (2013). Antibody to a conserved antigenic target is protective against diverse prokaryotic and eukaryotic pathogens. Proc. Natl. Acad. Sci. USA *110*, E2209–E2218.

Ding, J.W., Zhou, T., Zeng, H., Ma, L., Verbeek, J.S., Yin, D., Shen, J., and Chong, A.S. (2008). Hyperacute rejection by anti-Gal IgG1, IgG2a, and IgG2b is dependent on complement and Fc-gamma receptors. J. Immunol. *180*, 261–268.

Doenz, U., Nydegger, U.E., Kueng, A., Carrel, T., and Mohacsi, P. (2000). Anti-Galalpha1-3Gal IgM/IgG antibody levels in infants: do they have a clinical relevance in pediatric xenotransplantation? J. Heart Lung Transplant. *19*, 1108–1113.

Dolowy, W.C., and Muldoon, R.L. (1964). Studies of germfree animals. I. Response of mice to infection with influenza A virus. Proc. Soc. Exp. Biol. Med. *116*, 365–371.

Ehrenstein, M.R., O'Keefe, T.L., Davies, S.L., and Neuberger, M.S. (1998). Targeted gene disruption reveals a role for natural secretory IgM in the maturation of the primary immune response. Proc. Natl. Acad. Sci. USA *95*, 10089–10093.

Fagundes, C.T., Amaral, F.A., Vieira, A.T., Soares, A.C., Pinho, V., Nicoli, J.R., Vieira, L.Q., Teixeira, M.M., and Souza, D.G. (2012). Transient TLR activation restores inflammatory response and ability to control pulmonary bacterial infection in germfree mice. J. Immunol. *188*, 1411–1420.

Franke-Fayard, B., Trueman, H., Ramesar, J., Mendoza, J., van der Keur, M., van der Linden, R., Sinden, R.E., Waters, A.P., and Janse, C.J. (2004). A Plasmodium berghei reference line that constitutively expresses GFP at a high level throughout the complete life cycle. Mol. Biochem. Parasitol. *137*, 23–33.

Galili, U., and Swanson, K. (1991). Gene sequences suggest inactivation of alpha-1,3-galactosyltransferase in catarrhines after the divergence of apes from monkeys. Proc. Natl. Acad. Sci. USA *88*, 7401–7404.

Galili, U., LaTemple, D.C., and Radic, M.Z. (1998). A sensitive assay for measuring alpha-Gal epitope expression on cells by a monoclonal anti-Gal antibody. Transplantation *65*, 1129–1132.

Galili, U., Rachmilewitz, E.A., Peleg, A., and Flechner, I. (1984). A unique natural human IgG antibody with anti-alpha-galactosyl specificity. J. Exp. Med. *160*, 1519–1531.

Galili, U., Macher, B.A., Buehler, J., and Shohet, S.B. (1985). Human natural anti-alpha-galactosyl IgG. II. The specific recognition of alpha (1——3)-linked galactose residues. J. Exp. Med. *162*, 573–582.

Galili, U., Mandrell, R.E., Hamadeh, R.M., Shohet, S.B., and Griffiss, J.M. (1988). Interaction between human natural anti-alpha-galactosyl immunoglobulin G and bacteria of the human flora. Infect. Immun. 56, 1730–1737.

Gu, H., Zou, Y.R., and Rajewsky, K. (1993). Independent control of immunoglobulin switch recombination at individual switch regions evidenced through Cre-loxP-mediated gene targeting. Cell 73, 1155–1164.

Hayakawa, T., Satta, Y., Gagneux, P., Varki, A., and Takahata, N. (2001). Alu-mediated inactivation of the human CMP- N-acetylneuraminic acid hydroxylase gene. Proc. Natl. Acad. Sci. USA 98, 11399–11404.

Hegge, S., Kudryashev, M., Barniol, L., and Frischknecht, F. (2010). Key factors regulating Plasmodium berghei sporozoite survival and transformation revealed by an automated visual assay. FASEB journal 24, 5003–5012.

Honda, K., and Littman, D.R. (2012). The microbiome in infectious disease and inflammation. Annu. Rev. Immunol. 30, 759–795.

Huflejt, M.E., Vuskovic, M., Vasiliu, D., Xu, H., Obukhova, P., Shilova, N., Tuzikov, A., Galanina, O., Arun, B., Lu, K., and Bovin, N. (2009). Anti-carbohydrate antibodies of normal sera: findings, surprises and challenges. Mol. Immunol. 46, 3037–3049.

Ichinohe, T., Pang, I.K., Kumamoto, Y., Peaper, D.R., Ho, J.H., Murray, T.S., and Iwasaki, A. (2011). Microbiota regulates immune defense against respiratory tract influenza A virus infection. Proc. Natl. Acad. Sci. USA 108, 5354–5359.

Ishino, T., Orito, Y., Chinzei, Y., and Yuda, M. (2006). A calcium-dependent protein kinase regulates Plasmodium ookinete access to the midgut epithelial cell. Mol. Microbiol. 59, 1175–1184.

Kimmel, J., Ogun, S.A., de Macedo, C.S., Gerold, P., Vivas, L., Holder, A.A., Schwarz, R.T., and Azzouz, N. (2003). Glycosylphosphatidyl-inositols in murine malaria: Plasmodium yoelii yoelii. Biochimie 85, 473–481.

Lacroix-Desmazes, S., Mouthon, L., Coutinho, A., and Kazatchkine, M.D. (1995). Analysis of the natural human IgG antibody repertoire: life-long stability of reactivities towards self antigens contrasts with age-dependent diversification of reactivities against bacterial antigens. Eur. J. Immunol. 25, 2598–2604.

Luo, Y., Wen, J., Luo, C., Cummings, R.D., and Cooper, D.K. (1999). Pig xenogeneic antigen modification with green coffee bean alpha-galactosidase. Xenotransplantation 6, 238–248.

Macher, B.A., and Galili, U. (2008). The Galalpha1,3Galbeta1,4GlcNAc-R (alpha-Gal) epitope: a carbohydrate of unique evolution and clinical relevance. Biochim. Biophys. Acta 1780, 75–88.

Mañez, R., Blanco, F.J., Díaz, I., Centeno, A., Lopez-Pelaez, E., Hermida, M., Davies, H.F., and Katopodis, A. (2001). Removal of bowel aerobic gram-negative bacteria is more effective than immunosuppression with cyclophosphamide and steroids to decrease natural alpha-galactosyl IgG antibodies. Xenotransplantation 8, 15–23.

Ménard, R., Tavares, J., Cockburn, I., Markus, M., Zavala, F., and Amino, R. (2013). Looking under the skin: the first steps in malarial infection and immunity. Nat. Rev. Microbiol. 11, 701–712.

Miyatake, T., Sato, K., Takigami, K., Koyamada, N., Hancock, W.W., Bazin, H., Latinne, D., Bach, F.H., and Soares, M.P. (1998). Complement-fixing elicited antibodies are a major component in the pathogenesis of xenograft rejection. J. Immunol. 160, 4114–4123.

Modiano, D., Petrarca, V., Sirima, B.S., Nebié, I., Diallo, D., Esposito, F., and Coluzzi, M. (1996). Different response to Plasmodium falciparum malaria in west African sympatric ethnic groups. Proc. Natl. Acad. Sci. USA 93, 13206–13211.

Mombaerts, P., Clarke, A.R., Rudnicki, M.A., Iacomini, J., Itohara, S., Lafaille, J.J., Wang, L., Ichikawa, Y., Jaenisch, R., Hooper, M.L., et al. (1992). Mutations in T-cell antigen receptor genes alpha and beta block thymocyte development at different stages. Nature 360, 225–231.

Moran, P., and Caras, I.W. (1994). Requirements for glycosylphosphatidylinositol attachment are similar but not identical in mammalian cells and parasitic protozoa. J. Cell Biol. 125, 333–343.

Mota, M.M., Pradel, G., Vanderberg, J.P., Hafalla, J.C., Frevert, U., Nussenzweig, R.S., Nussenzweig, V., and Rodríguez, A. (2001). Migration of Plasmodium sporozoites through cells before infection. Science 291, 141–144.

Muramatsu, M., Kinoshita, K., Fagarasan, S., Yamada, S., Shinkai, Y., and Honjo, T. (2000). Class switch recombination and hypermutation require activation-induced cytidine deaminase (AID), a potential RNA editing enzyme. Cell 102, 553–563.

Nagele, E.P., Han, M., Acharya, N.K., DeMarshall, C., Kosciuk, M.C., and Nagele, R.G. (2013). Natural IgG autoantibodies are abundant and ubiquitous in human sera, and their number is influenced by age, gender, and disease. PLoS ONE 8, e60726.

Nimmerjahn, F., and Ravetch, J.V. (2008). Fcgamma receptors as regulators of immune responses. Nat. Rev. Immunol. 8, 34–47.

Olotu, A., Fegan, G., Wambua, J., Nyangweso, G., Awuondo, K.O., Leach, A., Lievens, M., Leboulleux, D., Njuguna, P., Peshu, N., et al. (2013). Four-year efficacy of RTS,S/AS01E and its interaction with malaria exposure. N. Engl. J. Med. 368, 1111–1120.

Oyelaran, O., McShane, L.M., Dodd, L., and Gildersleeve, J.C. (2009). Profiling human serum antibodies with a carbohydrate antigen microarray. J. Proteome Res. 8, 4301–4310.

Pal, S.C., Rao, C.K., Kereselidze, T., Krishnaswami, A.K., Murty, D.K., Pandit, C.G., and Shrivastav, J.B. (1969). An extensive community outbreak of enteropathogenic Escherichia coli O86: B7 gastroenteritis. Bull. World Health Organ. 41, 851–858.

Parker, W., Lin, S.S., Yu, P.B., Sood, A., Nakamura, Y.C., Song, A., Everett, M.L., and Platt, J.L. (1999). Naturally occurring anti-alpha-galactosyl antibodies: relationship to xenoreactive anti-alpha-galactosyl antibodies. Glycobiology 9, 865–873.

Porcherie, A., Mathieu, C., Peronet, R., Schneider, E., Claver, J., Commere, P.H., Kiefer-Biasizzo, H., Karasuyama, H., Milon, G., Dy, M., et al. (2011). Critical role of the neutrophil-associated high-affinity receptor for IgE in the pathogenesis of experimental cerebral malaria. J. Exp. Med. 208, 2225–2236.

Posekany, K.J., Pittman, H.K., Bradfield, J.F., Haisch, C.E., and Verbanac, K.M. (2002). Induction of cytolytic anti-Gal antibodies in alpha-1,3-galactosyltransferase gene knockout mice by oral inoculation with Escherichia coli O86:B7 bacteria. Infect. Immun. 70, 6215–6222.

Rickman, L.S., Jones, T.R., Long, G.W., Paparello, S., Schneider, I., Paul, C.F., Beaudoin, R.L., and Hoffman, S.L. (1990). Plasmodium falciparum-infected Anopheles stephensi inconsistently transmit malaria to humans. Am. J. Trop. Med. Hyg. 43, 441–445.

Ringel-Kulka, T., Cheng, J., Ringel, Y., Salojärvi, J., Carroll, I., Palva, A., de Vos, W.M., and Satokari, R. (2013). Intestinal microbiota in healthy U.S. young children and adults—a high throughput microarray analysis. PLoS ONE 8, e64315.

Sauerwein, R.W., Roestenberg, M., and Moorthy, V.S. (2011). Experimental human challenge infections can accelerate clinical malaria vaccine development. Nat. Rev. Immunol. 11, 57–64.

Seder, R.A., Chang, L.J., Enama, M.E., Zephir, K.L., Sarwar, U.N., Gordon, I.J., Holman, L.A., James, E.R., Billingsley, P.F., Gunasekera, A., et al.; VRC 312 Study Team (2013). Protection against malaria by intravenous immunization with a nonreplicating sporozoite vaccine. Science 341, 1359–1365.

Springer, G.F., and Horton, R.E. (1969). Blood group isoantibody stimulation in man by feeding blood group-active bacteria. J. Clin. Invest. 48, 1280–1291.

Springer, G.F., Horton, R.E., and Forbes, M. (1959). [Origin of anti-human blood group B agglutinins in white Leghorn chicks]. J. Exp. Med. 110, 221–244.

Takahashi, H., Chinuki, Y., Tanaka, A., and Morita, E. (2014). Laminin γ-1 and collagen α-1 (VI) chain are galactose-α-1,3-galactose-bound allergens in beef. Allergy 69, 199–207.

Takeuchi, Y., Porter, C.D., Strahan, K.M., Preece, A.F., Gustafsson, K., Cosset, F.L., Weiss, R.A., and Collins, M.K. (1996). Sensitization of cells and retroviruses to human serum by (alpha 1-3) galactosyltransferase. Nature 379, 85–88.

Tangvoranuntakul, P., Gagneux, P., Diaz, S., Bardor, M., Varki, N., Varki, A., and Muchmore, E. (2003). Human uptake and incorporation of an immunogenic nonhuman dietary sialic acid. Proc. Natl. Acad. Sci. USA *100*, 12045–12050.

Tearle, R.G., Tange, M.J., Zannettino, Z.L., Katerelos, M., Shinkel, T.A., Van Denderen, B.J., Lonie, A.J., Lyons, I., Nottle, M.B., Cox, T., et al. (1996). The alpha-1,3-galactosyltransferase knockout mouse. Implications for xenotransplantation. Transplantation *61*, 13–19.

Tran, T.M., Ongoiba, A., Coursen, J., Crosnier, C., Diouf, A., Huang, C.Y., Li, S., Doumbo, S., Doumtabe, D., Kone, Y., et al. (2014). Naturally acquired antibodies specific for Plasmodium falciparum reticulocyte-binding protein homologue 5 inhibit parasite growth and predict protection from malaria. J. Infect. Dis. *209*, 789–798.

Verhage, D.F., Telgt, D.S., Bousema, J.T., Hermsen, C.C., van Gemert, G.J., van der Meer, J.W., and Sauerwein, R.W. (2005). Clinical outcome of experimental human malaria induced by Plasmodium falciparum-infected mosquitoes. Neth. J. Med. *63*, 52–58.

Warburg, A., Shtern, A., Cohen, N., and Dahan, N. (2007). Laminin and a Plasmodium ookinete surface protein inhibit melanotic encapsulation of Sephadex beads in the hemocoel of mosquitoes. Microbes Infect. *9*, 192–199.

Weiss, W.R., Good, M.F., Hollingdale, M.R., Miller, L.H., and Berzofsky, J.A. (1989). Genetic control of immunity to Plasmodium yoelii sporozoites. J. Immunol. *143*, 4263–4266.

Yang, Y.G., deGoma, E., Ohdan, H., Bracy, J.L., Xu, Y., Iacomini, J., Thall, A.D., and Sykes, M. (1998). Tolerization of anti-Galalpha1-3Gal natural antibody-forming B cells by induction of mixed chimerism. J. Exp. Med. *187*, 1335–1342.

Yi, W., Bystricky, P., Yao, Q., Guo, H., Zhu, L., Li, H., Shen, J., Li, M., Ganguly, S., Bush, C.A., and Wang, P.G. (2006). Two different O-polysaccharides from Escherichia coli O86 are produced by different polymerization of the same O-repeating unit. Carbohydr. Res. *341*, 100–108.

Yin, D., Zeng, H., Ma, L., Shen, J., Xu, H., Byrne, G.W., and Chong, A.S. (2004). Cutting edge: NK cells mediate IgG1-dependent hyperacute rejection of xenografts. J. Immunol. *172*, 7235–7238.

EXTENDED EXPERIMENTAL PROCEDURES

Material

Synthetic α-gal linked to bovine serum albumin (BSA) or human serum albumin (HSA; Dextra Labs; Reading, UK), α-galactosidase from green coffee beans (Sigma Chemical Co), Fluorescein isothiocyanate (FITC)-conjugated (Sigma-Aldrich Co) and Alexa Fluor 647-conjugated (Invitrogen) *Bandeiraea simplicifolia* lectin (BSI-IB$_4$; *Griffonia simplicifolia*) (Kisailus and Kabat, 1978), rabbit RBC (Patricell Ltd.; Nottingham, UK), incomplete Freund's Adjuvant (IFA) (BD Difco), inactivated and dried *M. tuberculosis* H37 Ra (BD Difco), Dextran, Tetramethylrhodamine, 10,000 MW, Lysine Fixable (fluoro-Ruby; Life Technologies), mouse anti-α-gal IgM (M86; EnzoLife Sciences or kindly provided by Uri Galili, University of Massachusetts Medical School, Worcester, MA, USA) (Galili et al., 1998), IgG1 (GT6-27), IgG2a, IgG2b and IgG3 (GT4-31) mAbs (Ding et al., 2008; Yin et al., 2004), mouse anti-dinitrophenyl IgM (MADNP-5), IgG1 (MADNP-1), IgG2a (MADNP-2), IgG2b (MADNP-3) and IgG3 (MADNP-4) mAbs (kindly provided Hérve Bazin, University of Louvain, Belgium) (Platteau et al., 1990). Mouse IgM, IgG1, IgG2a, IgG2b, IgG3, IgA and IgE were detected using horse-radish peroxidase (HRP)-conjugated goat anti-mouse IgM, IgG1, IgG2a, IgG2b, IgA and IgE or a rat mAb anti-mouse IgG3 (Southern Biotechnology Associates). Anti-CSP 3D11 (Yoshida et al., 1980) hybridoma (IgG1 mAb directed against the repeat region of *P. berghei* CSP) was kindly provided by Ana Rodriguez (New York Medical School).

Cohort Study

The Ethics Committee of the Faculty of Medicine, Pharmacy and Dentistry at the University of Sciences, Technique and Technology of Bamako, and the Institutional Review Board of NIAID-NIH approved the cohort study. In May 2011, 695 individuals aged 3 months to 25 years were enrolled in a cohort study in the rural village of Kalifabougou, Mali. Individuals were followed during the malaria season for 7 months. Individuals were invited to participate after random selection from an age-stratified census of the entire village population (n = 4394). Written, informed consent was obtained from adult participants and the parents or guardians of participating children. Enrollment exclusion criteria were hemoglobin level < 7 g/dL, axillary temperature $\geq 37.5°C$, acute systemic illness, use of anti-malarial or immunosuppressive medications in the past 30 days and pregnancy. Clinical malaria was detected prospectively by self-referral and weekly active clinical surveillance. All individuals with signs and symptoms of malaria and any level of *Plasmodium* parasitemia detected by light microscopy were treated according to the National guidelines in Mali. The research definition of malaria was parasitemia ≥ 2500 parasites/μL, temperature $\geq 37.5°C$ and no other cause of fever discernible by physical exam. During scheduled clinic visits, blood was collected by finger prick every two weeks on filter paper. Detection of asymptomatic *Plasmodium* infection by PCR was done retrospectively at the end of the surveillance period. For each participant, PCR was performed on blood samples in chronological order from enrollment onward until the first *P. falciparum* infection was detected. Detailed methods for *P. falciparum* PCR detection have been described (Tran et al., 2013). α-gal-specific IgM and IgG Ab levels were determined using ELISA on plasma collected at enrollment from the subset of individuals. Statistical analyses were described in the Statistical analysis' section.

Genotyping

Mice were genotyped by PCR using tail genomic DNA and the following primers: i) $\alpha 1,3Gt^{-/-}$: 5′-TCTTGACGAGTTCTTCTGAG-3′, 5′-TCAGCATGATGCGCATGAAGA-3′, 5′-TGGCCGCGTGGTAGTAAAAA-3′; ii) $J_HT^{-/-}$: 5′-CAGTGAATGACAGATGGACCTCC-3′, 5′-G CAGAAGCCACAACC ATACATTC-3′, 5′-ACAGTAACTCGTTCTTCTCTGC-3′; iii) $Aid^{-/-}$: 5′-GGCCAGCTCATTCCTCCACT-3′, 5′-CAC TGAGCGCACCTGTAGCC-3′, 5′-CCTAGTGGCCAAGGTGCAGT-3′, 5′-TCAGGCTGAGGTTAGGGTTCC-3′; iv) $Tcr\beta^{-/-}$: 5′-TGTCT GAAGGGCAATGACTG-3′, 5′-GCTGATCCGTGGCATCTATT-3′, 5′-CTTGGGTGGAGAGGCTATTC-3′, 5′-AGGTGAGATGACAGGAG ATC-3′; v) $C3^{-/-}$: 5′-ATCTTGAGTGCACCAAGCC-3′, 5′-GGTTGCAGCAGTCTATGAAGG-3′, 5′-GCCAGAGGCCACTTGTGTAG-3′. $\mu S^{-/-}$ mice were phenotyped by ELISA, as described (Ehrenstein et al., 1998). Total genomic DNA was isolated from the tail using a standard protocol. Briefly, tails (0,5 to 1 cm) were obtained and submerged into DirectPCR Lysis Reagent (200-300 μL; Viagen Biotech) containing Proteinase K (100 μg/ml) and incubated (overnight; 55°C) under vigorous agitation. Next day, samples were centrifuged (16,000 g; 5-10 s; RT) and supernatant (1 μl) was amplified by PCR: 95°C (15 min), 30 cycles of 94°C (45 s), 60°C (90 s) (except $Aid^{-/-}$ genotyping; 63°C), 72°C (90 s) and 72°C (15 min). Visualizations of PCR results were done on 1.5%–2% agarose gel (80-100V; 1-2 hr).

Extraction of Rabbit RBC Membranes

Rabbit RBC membranes (rRBCM) expressing high levels of α-gal (Eto et al., 1968) were prepared from lyzed RBC (50 mM sodium phosphate buffer pH 8), washed (5-7X; sodium phosphate buffer; 10,000 g; 20 min, 4°C) until supernatant was hemoglobin-free, essentially as described (Matsuzawa and Ikarashi, 1979). Membranes were collected by centrifugation (20,000 g; 20 min, 4°C), re-suspended in PBS and stored (−80°C) until used.

Immunization

rRBCM were emulsified in Complete Freund's Adjuvant (CFA; Incomplete Freund's Adjuvant (IFA) plus *Mycobacterium tuberculosis* H37 RA; 4 mg/ml; DIFCO) with CpG (50 μg/mouse; ODN M362; Invivogen) and administered subcutaneously (s.c.). Two subsequent immunizations were emulsified in IFA+rRBC+CpG. Emulsions were administered at 200 μl per mouse, 3 times at two weeks intervals.

Mice were also immunized (s.c.) with α-gal-BSA (75 μg/mouse) emulsified in CFA with two subsequent immunizations, 2 and 4 weeks thereafter with α-gal-BSA emulsified in IFA.

Anti-α-Gal ELISA

Mouse serum was collected two weeks after immunization and circulating anti-α-gal antibodies were quantified by ELISA, as described (Galili et al., 1998; LaTemple and Galili, 1998). Briefly, 96-well plates (PolySorp; Nunc) were coated with α-gal (α-gal-HSA or α-gal-BSA; 50 μl; 10 μg/ml in 0.5 M carbonate bicarbonate buffer; pH 9.5; 2 hr at 37°C or overnight at 4°C), blocked with BSA (100 μl; 1% w/v in PBS; 1 hr; RT) and washed (5X; PBS/0.05% Tween-20). Plates were incubated (1 hr; RT) with serum serial dilutions in PBS, 1% BSA and washed (5X; PBS/0.05% Tween-20). Anti-α-gal antibodies were detected using HRP-conjugated anti-mouse IgM, total IgG, IgG1, IgG2a, IgG2b or IgG3 (50 μl, 1:1-2,000 dilution, 1 hr, RT) and washed (5X; PBS/0.05% Tween-20). Purified anti-α-gal IgM (Galili et al., 1998), IgG1 (GT6-27), IgG2a and IgG2b and IgG3 (GT4-31) mAb (Ding et al., 2008; Yin et al., 2004) were used as standards. TMB Substrate Reagent Set (BD Biosciences) was used to reveal peroxidase activity (15-30 min; RT) and the reaction was stopped using 2N sulfuric acid. Optical densities (OD) were reported at λ = 450 nm and normalized by subtracting background OD values (λ = 600 nm) (Victor 3; PerkinElmer). Concentration of each anti-α-gal IgG subclass was determined, as described (Spalter et al., 1999). Concentration of anti-α-gal antibodies in human plasma was analyzed using a similar assay and a standard curve to transform absorbance into immunoglobulin concentration was obtained by coating 8 duplicate wells in every plate with purified human IgG and IgM (500 to 1.5 ng/ml) and performing the protocol described above in the absence of diluted serum.

Anti-α-Gal mAbs

Anti-α-gal hybridomas were cultured in RPMI 1640 (Invitrogen Life Technologies) supplemented with 0.1 mM Sodium Pyruvate, 0.01 M HEPES, 0.05 mM 2-mercaptoethanol and 2% FBS (IgG depleted). Anti-α-gal IgG2a, IgG2b and IgG3 hybridomas were derived by sub-cloning of the original IgG1 (GT6-27) hybridoma and as such have similar affinities for α-gal, as described (Ding et al., 2008; Yin et al., 2004). Antibodies were purified by affinity chromatography using HiTrap Protein G columns (GE Healthcare Life Sciences). Anti-α-gal IgG3 purification was carried out by a nonchromatographic method taking advantage of its euglobulin properties, as described (García-González et al., 1988). Purified mAbs were extensively dialyzed against PBS. Protein concentration was determined using NanoDrop ND-1000 spectrophotometer (λ = 280 nm; Thermo Scientific) and purity confirmed by SDS-PAGE analysis. When indicated, mAbs were labeled with Alexa Fluor 647 Protein Labeling Kit (A20173), as per manufacturer recommendations (Molecular Probes, Invitrogen). Anti-mouse IgM total-A647 (Clone: R33.24.12) was used to reveal anti-α-gal IgM mAb in immunofluorescence assay.

Passive Anti-α-Gal mAbs Transfer

$\alpha1,3Gt^{-/-}$ mice received anti-α-gal IgG1, IgG2a, IgG2b or IgG3 mAbs via a single i.v. injection (150 μg; 100 μl per mouse), 24 hr prior to mosquito exposure. Passive anti-α-gal IgM transfer was performed using polyclonal IgM. Briefly, eight to ten weeks old $\alpha1,3G^{-/-}Aid^{-/-}$ mice received 3×10^8 RBC equivalents of rRBCM in PBS (100 μl; i.p.). Serum was collected two weeks after the last immunization and concentration of anti-α-gal IgM was determined by ELISA (Galili et al., 1998; LaTemple and Galili, 1998). Serum collected from naive $\alpha1,3G^{-/-}Aid^{-/-}$ mice was used as control. $\alpha1,3Gt^{-/-}$ mice received the polyclonal IgM via a single i.v. (150 μg; 300-400 μl per mouse), 24 hr prior to mosquito exposure.

Plasmodium Strains

For sporozoite production, *P. berghei* ANKA infected RBC (1×10^6) were administered i.p. to BALB/c mice and the presence of gametocyte-stage parasites capable of exflagellation was monitored in fresh blood preparations. Infected BALB/c mice were used to feed 3 to 4-day-old female mosquitoes (~1 hr), which were used 18-25 days postinfection for subsequent infections. When infected with *P. berghei* ANKA mosquitoes were maintained at 21°C (IHMT) whereas mosquitoes infected with *P. yoelii* 17XNL-GFP(Ono et al., 2007) were maintained (24-25°C; Centre for Production and Infection of *Anopheles*; CEPIA, Pasteur Institute, France). Alternatively, *P. yoelii* 17XNL (MR4; MRA-593) (Weiss et al., 1989) infected mosquitoes were purchased from Radboud University Nijmegen Medical Centre (Nijmegen, Netherlands). *P. falciparum* 3D7 strain (kindly provided by Robert Menard, Institut Pasteur, France) (Walliker et al., 1987) were used for α-gal detection in infected RBC by immunofluorescence assay.

Sporozoites Isolation and Inoculation

Mosquitoes were narcotized (−20°C; 3-5 min), washed in 70% ethanol (1X; 10-20 s) and PBS (3X; 10-20 s; Ambion). Salivary glands were obtained by dissection under a zoom stereomicroscope (3X magnification; Nikon SMZ800, Japan) and preserved in RPMI 1640 medium (GIBCO BRL) or PBS. Salivary glands were smashed using Pellet pestles cordless motor (10-15 s; Sigma) to release sporozoites and centrifuged (100 g; 5 min) in LoBind microfuge tubes (Eppendorf). Supernatant was filtered (100 μm cell strainers; BD Falco) to exclude debris. Sporozoites were counted using KOVA Glasstic Slide 10 with quantitative grid (Fisher Scientific GMBH). $PbA^{EEF1a-GFP}$ sporozoites were inoculated i.d. in the ear pinna (750 sporozoites in 20-30 μl; 1% BSA in PBS) or i.v. (retro-orbital; 150 sporozoites in 50 μl; 1% BSA in PBS) using a microsyringe (Nanofil 100 μl; 33G beveled needle; World Precision Instruments).

Passive RBCs Transfer

$\alpha 1,3Gt^{-/-}$ mice immunized with rRBCM and age matched naive $\alpha 1,3Gt^{-/-}$ mice were exposed to PbA$^{EEF1a-GFP}$ infected mosquitoes, as described above. Parasitemia was monitored by flow cytometry in FacScan analyzer (BD Biosciences). Nine days post-mosquito feeding, blood was collected and injected i.p. (100-200 μl) to naive $\alpha 1,3Gt^{-/-}$ mice. Infection was monitored daily for parasitemia and clinical symptoms, starting from day 3–4 postinfection RBC administration.

Quantification of Sporozoite mRNA

The mouse ear was excised immediately after and the whole liver was harvested 40 hr after mosquito biting. Samples were frozen in liquid nitrogen, tissues were homogenized in TRIzol (Life Technologies), total RNA isolated according to manufacturer's instructions (RNeasy Mini kit; QIAGEN). Briefly, RNA (2 μg; 10 μl) was mixed to random primers (1 μl) and dNTPs (10 mM; 1 μl), incubated (65°C; 5 min.), placed on ice and incubated in PCR Buffer (0.1 M DTT; 40 units/μl RNaseOU; 2 min.; 42°C). Superscript RT (SSIIRT) was added (1 μl; 50 min. 42°C) and samples were heated to finalize synthesis (70°C; 15 min). qRT-PCR was performed using PbA 18S rRNA specific primers (5′-AAGCATTAAATAAAGCGAATACATCCTTAC-3′ and 5′-GGAGA TTGGTTTTGACGTTTATGTG-3′). Mouse housekeeping $Arbp0$ gene (5′-CTTTGGGCATCACCACGAA-3′ and 5′-GCTGGCTCCCACCTTGTCT-3′) was amplified as control. Applied Biosystems' Power SYBR Green PCR Master Mix was used as per manufacturer's instructions (ABI Prism 7000 system; Applied Biosystems). Data are presented as relative expression of $P.\ berghei$ ANKA 18S rRNA normalized to mouse $Arbp0$ mRNA.

Detection of α-Gal in $Plasmodium$ Sporozoites

PbA$^{EEF1a-GFP}$, PbA$^{Hsp70-GFP}$, $P.\ falciparum$ 3D7 or $P.\ yoelii$ 17XNL-GFP sporozoites, isolated from the salivary glands of $Anopheles$ $stephensi$ or $Anopheles\ gambiae$ mosquitoes, 18-25 days postinfection were allowed to attach to Teflon printed (10 wells, 8 mm; no-adherent surface; Immuno-Cell Int.) or to diagnostic glass slides. Sporozoites were fixed (20-50 μl; 4% PFA; 20-30 min; RT or 37°C) and washed gently (1X; PBS). Sporozoites were stained with Alexa Fluor 647 conjugated BSI-IB$_4$ (100 μl; 200 μg/ml; 2 hr, RT), Alexa Fluor 647 conjugated anti-α-gal IgG1, IgG2a, IgG2b, IgG3 mAb (100 μl; 50 μg/ml; overnight; 4°C) or with nonconjugated anti-α-gal IgM (M86) mAb (100 μl; 50 μg/ml; overnight; 4°C) and washed (1X; PBS). Nonconjugated IgM antibodies were detected using Alexa Fluor 647 conjugated goat anti-mouse IgM (100 μl; 10 μg/ml; overnight, 4°C) (Molecular Probes, Invitrogen). After washing (1X; PBS), slides were incubated with 4',6-diamidino-2-phenylindole (DAPI) (100 μl; 10 μg/ml; 10 min; RT) (Molecular Probes, washed (1X; PBS) and dried in dark room without covering with coverslip (RT). Images of PbA sporozoites were obtained by DeltaVision Core immunofluorescence microscopy (Applied Precision/Olympus) or Spinning Disk Confocal microscopy Revolution xD (Andor Technology) at 100 × magnification. Actin was detected using Alexa Fluor 488 Phalloidin (Molecular Probes; 100 μl; 3 units/ml; 1 hr; RT) in $P.\ falciparum$ 3D7 and $P.\ yoelii$ 17XNL-GFP sporozoites to which was added ProLong Gold Antifade Reagent (Invitrogen) and wells were covered with coverslips. Slides were visualized with Axiovert II fluorescence microscope (Zeiss). Images were analyzed using bicubic interpolation and rescaling with ImageJ software (NIH).

For detection of α-gal by flow cytometry, PbA$^{Hsp70-GFP}$ sporozoites were isolated from the salivary glands of $A.\ stephensi$ mosquitoes 19-25 days postinfection (10^5; 30-40ul; PBS; ice cold: 30 min), fixed (30-40 μl; 4% PFA in PBS; 20-30 min; 37°C) and washed (1 × ; PBS; 9,300 g; 2 min). Staining was performed with Alexa Fluor 647 conjugated BSI-IB$_4$ (100 μg/ml; 1 hr; 37°C). Sporozoites were washed (1 × ; PBS; 9,300 g; 2 min) and Alexa Fluor 647 BSI-IB$_4$ signal was detected in CyAn^{TM} ADP flow cytometry (Beckman Coulter; USA) with Summit Software (v4.3; Beckman Coulter), gating on FITC (for sporozoite detection) and APC (for α-gal detection).

For detection of α-gal by western blotting PbA$^{Hsp70-GFP}$, $P.\ falciparum$ 3D7 and $P.\ yoelii$ 17XNL-GFP sporozoites were isolated from the salivary glands of 40-70 mosquitoes, 21-25 days after infection. Briefly, salivary glands were collected into the LoBind microfuge tubes (PBS; on ice), smashed using pellet pestles cordless motor (10-15 s; 2X) and a short spin was applied to pellet debris. Supernatant (30-50 μl; 1-2.5 × 10^5 sporozoites) was transferred into LoBind microfuge tube and aliquots were stored at −80°C until used. Number of $Plasmodium$ sporozoites (equivalent to 10^5 per sample) was normalized to corresponding number of salivary glands from noninfected mosquitoes. Samples were lysed (50 mM Tris/HCl pH 7.5, 150 mM NaCl, 1% Triton X-100, Roche complete EDTA-free protease inhibitor cocktail; 1 hr; on ice) and centrifuged (16,000 g, 10 min.; 4°C). Samples (supernatant) were denatured with Laemmli buffer (1% β-mercaptoethanol; 2%SDS; 95°C; 2 min) and separated in SDS-PAGE gradient gel (12% acrylamide/bisacrylamide gel, 29:1; 100V; 2 hr). Proteins were transferred into a PVDF membrane (90 min; 12V), blocked (3% BSA) and incubated overnight with anti-α-gal IgG2b mAb (1 μg/ml; 20 ml). Membrane was washed with 20 mM Tris/HCl pH7.5, 150 mM NaCl and 0.1% Tween-20 buffer (TBST, 3 × ; 5 min; RT) and incubated with horseradish peroxidase (HRP)-conjugated goat anti-mouse IgG2b-HRP (SouthernBiotech, 20 ng/ml; 1 hr; 50 ml; RT). Membrane was washed (TBST; 1 hr; RT) and developed (SuperSignal Chemiluminescent detection kit; West Pico, Thermo Scientific).

GPI Anchor Cleavage from $Plasmodium$ Sporozoites

PbA$^{Hsp70-GFP}$ sporozoites were fixed (4% PFA in PBS; 20-30 min; 37°C) and treated with phosphatidylinositol-specific phospholipase C (from $Bacillus\ cereus$; 5U/ml; 14-16 hr; 37°C). Detection of α-gal is described above and CSP was detected using anti-CSP conjugated to Alexa Fluor 647 in CyA ADP Analyzer (Beckman Coulter).

Bacterial Strains and Growth Conditions

Frozen $E.\ coli$ O86:B7 (ATCC 12701^{TM}; Rockville, Md.) and $E.\ coli$ K12 (ATCC 10798) (∼10^7 CFU/ml; 50% glycerol solution; −80°C) stocks were inoculated into Luria broth (LB; 50 ml; 37°C; overnight) on a shaker rack. Spectrophotometric absorbance was measured

at 600 nm (Optical Density-OD_{600}) and adjusted to OD_{600} ~0.2 in order to harvest bacteria during exponential growth corresponding to a OD_{600} of 2. The approximate cell number was determined according to spectrophotometric measurement and confirmed with most probable numbers (MPN) technique, also known as the method of Poisson zeroes (Oblinger and Koburger, 1975).

Detection of α-Gal on Bacterial Cultures

E. coli O86:B7 and *E.coli* K12 were cultured (LB; 50 ml; 37°C; overnight), washed (2 × ; PBS; 4,000 g; 5 min; 4°C) and re-suspended in PBS. Bacteria were fixed (200 μl; 4% PFA in PBS; 20-30 min; RT) and washed (1X; PBS; 4000 g; 5 min; RT). 10^8-10^9 CFU/ml were stained with $BSI-IB_4$-FITC (200 μl; 50 μg/ml; 2 hr, RT) for flow cytometry analysis using FacScan analyzer (BD Biosciences). In parallel, immunofluorescence assays were performed using 10 μl stained samples after air-drying (10-20 min; RT). Samples were washed (1x; PBS), incubated with 4',6-diamidino-2-phenylindole (DAPI) (200 μl; 10 μg/ml; 10 min; RT; Molecular Probes) and washed (1 × ; PBS). Immunofluorescence images were obtained by Spinning Disk Confocal microscopy Revolution xD (Andor Technology; USA) at 100 × magnification and images were processed with ImageJ (NIH) software.

Rederivation of GF α1,3Gt$^{−/−}$ Mice

Briefly, pregnant female *α1,3Gt$^{−/−}$* mice were euthanized (20 days postcoitum), uteri were immersed in 1% VirkonS, rinsed in sterile water and pups were transferred to surrogate mothers kept in GF isolators (Gettinge-La Calhéne, France). GF status was monitored every third week onward.

Gnotobiotic and SPF-Colonized Mice

α1,3Gt$^{−/−}$ mice were re-derived via caesarean section from SPF into GF conditions at the Instituto Gulbenkian de Ciência, as described (http://strains.emmanet.org/protocols/GermFree_0902.pdf). For gnotobiotic colonization, 8-12 weeks GF *α1,3Gt$^{−/−}$* mice were transferred into sterile micro isolator Ventiracks (Biozone, Margate, UK), fed *ad libitum* with a standard autoclaved chow diet and water and GF status was monitored every third week onward. GF and SPF *α1,3Gt$^{−/−}$* mice treated with streptomycin sulfate (5 g/l in drinking water for 7 days; GIBCO), were starved for 12 hr and colonized with *E. coli* O86:B7 or *E. coli* K12 (~10^7 CFU/100 μl Luria-Bertani - LB - medium) via oral gavage, using a 20-gauge stainless steel animal feeding needle (Cadence Science, Japan). Control mice were inoculated with sterile LB medium. Colonization protocol was administered 3 times at two weeks intervals.

Complement Activation

*Pb*A$^{Hsp70-GFP}$ sporozoites were exposed to anti-α-gal mAbs (150 μg/ml; in 50 μl DMEM; 60 min; 4°C) and subsequently to naive C57BL/6 mouse plasma (1:5 in 0.1% gelatin in Veronal Buffer (VB)$^{2+}$; 50 μl; 60 min; 37°C) (Lonza), used as a source of complement. Samples were washed (1 × ; PBS). C3 was detected using APC labeled anti-C3/C3b/iC3b (Clone: 6C9; 1:100; 50 μl; 45 min; 4°C) and analyzed in CyA ADP Analyzer (Beckman Coulter).

Sporozoite Cytotoxicity Assays

*Pb*A$^{Hsp70-GFP}$ sporozoites ($10-50x10^3$) were incubated with anti-α-gal or isotype matched anti-DNP mAbs (150 μg/ml mAb in 10 μl DMEM GlutaMA; 60 min; 4°C). Naive C57BL/6 mouse plasma (1:5) or baby rabbit complement (1:10; Cedarlane Laboratories) was added (0.1% gelatin in VB^{2+}) as a source of complement (60 min; 37°C). Cytotoxicity was quantified according to GFP expression in Andor Spinning Disk Confocal Microscopy (Andor Technology). Alternatively, *Pb*A$^{EEF1a-GFP}$ sporozoites ($10-30 × 10^3$) were isolated from the salivary glands of *Anopheles stephensi* mosquitoes, 19-25 days postinfection and incubated with anti-α-gal or isotype matched anti-DNP mAbs (150 μg/ml mAb in 10 μl PBS, Life Technologies) (60 min; on ice). Plasma from C57BL/6 mice (1:5) or baby rabbit complement (bRC; 1:10; Cedarlane Laboratories) was added (0.1% gelatin in VB^{2+} buffer; Lonza) as a source of complement (60 min; 37°C). Alternatively, sporozoite cytotoxicity was evaluated according to loss of crescent-shaped morphology (%).

Invasion Assay

Human hepatoma cells (HepG2; kindly provided from Robert Menard, Institut Pasteur, France) were cultured ($4x10^4$/well; 200 μl in 96-well plates) in DMEM (GlutaMA, 10% FBS, 100U/ml penicillin/streptomycin; Life Technologies) (37°C; 5%CO_2; 2 days). *Pb*A$^{Hsp70-GFP}$ sporozoites (19-25 days postinfection) were preincubated with anti-α-gal or isotype matched control anti-DNP mAbs (150 μg/ml in 20-50 μl; 60 min; 4°C). Plasma from C57BL/6 mice (1:5 in 20-50 μl 0.1% gelatin in VB^{2+} buffer; Lonza) was added (60 min.; 37°C) as a source of complement and sporozoites were immediately transferred onto HepG2 cells at a 1:4 parasite/cell ratio. Cocultures were incubated (120 min; 37°C) with Tetramethylrhodamine-Dextran (10,000 MW, 1:1; 2 mg/ml; Molecular Probes), washed (2X; PBS) and trypsinized (30-50 μl; 0.05% Trypsin-EDTA (1X), phenol red (GIBCO). Percentage of wounded and parasite-invaded cells was determined by flow cytometry analysis (FACScan, BD Biosciences), gating on FL1 (GFP; invasion) and FL2 (Dextran-Red; wounding). Sporozoite maturation was determined by quantifying the number of EEFs per field and EEF area after 40 hr coculture in 15 μ-Slide 8 well (ibiTreat; IBIDI; Germany) using fluorescence microscopy (Screening Microscopy; Nikon Eclipse TE2000-S). Images were obtained at 20x magnification. Pictures were analyzed using Image J software (NIH).

PMN Cell Depletion

Anti-Gr1 mAb (Clone: RB6-8C5; RB6-8C5 hybridoma) was produced at the IGC under serum-free conditions using a CELLine (Integra, Switzerland) (Tepper et al., 1992). Neutrophils were depleted in $\alpha1,3Gt^{-/-}$ mouse by a single intravenous anti-Gr1 mAb injection (250 μg), 48 hr prior to mosquito biting. PMN depletion was confirmed by staining for CD11b-FITC (Integrin α[M] chain, Mac-1 α chain, CR3, BD PharMingen^{TM}) and Anti-Gr1-PE (1A8, BD PharMingen^{TM}) and analyzed in flow cytometry(Tsiganov et al., 2014) (CyA ADP Analyzer, Beckman Coulter).

Statistical Analysis

All tests (except human cohort studies) were performed using the GraphPad Prism v6.0 (GraphPad Software). Human analyses were performed in R version 3.0.2 (http://www.R-project.org). Ab levels between groups were compared with the Kruskal-Wallis test. The relationship between Ab levels and time to *P. falciparum* infection and febrile malaria was determined by Kaplan-Meier survival analysis and the log-rank test. Age dependent differences in anti-α-gal IgM and IgG antibody concentrations in human serum were determined using nonparametric Mann-Whitney test. Differences in anti-α-gal antibody concentration in mouse serum were determined using nonparametric Kruskal-Wallis test with Dunn's multiple comparison posttest. Incidence of infection was compared using log rank (Mantel-Cox) test. Survival curves were plotted using Kaplan-Meier plot and significant differences among experimental groups were determined using the Log-Rank (Mantel-Cox) test. Data corresponding to relative amount of *Plasmodium* in the skin and liver obtained from qRT-PCR was analyzed using nonparametric Mann–Whitney test. Cytotoxic effect of anti-α-gal antibodies was analyzed using repeated-measures ANOVA followed by Tukey's multiple comparison posttest. A p value equal to or below 0.05 was considered statistically significant.

SUPPLEMENTAL REFERENCES

Circolo, A., Garnier, G., Fukuda, W., Wang, X., Hidvegi, T., Szalai, A.J., Briles, D.E., Volanakis, J.E., Wetsel, R.A., and Colten, H.R. (1999). Genetic disruption of the murine complement C3 promoter region generates deficient mice with extrahepatic expression of C3 mRNA. Immunopharmacology *42*, 135–149.

Eto, T., Ichikawa, Y., Nishimura, K., Ando, S., and Yamakawa, T. (1968). Chemistry of lipid of the posthemyolytic residue or stroma of erythrocytes. XVI. Occurrence of ceramide pentasaccharide in the membrane of erythrocytes and reticulocytes of rabbit. J. Biochem. *64*, 205–213.

García-González, M., Bettinger, S., Ott, S., Olivier, P., Kadouche, J., and Pouletty, P. (1988). Purification of murine IgG3 and IgM monoclonal antibodies by euglobulin precipitation. J. Immunol. Methods *111*, 17–23.

Kisailus, E.C., and Kabat, E.A. (1978). A study of the specificity of Bandeiraea simplicifolia lectin I by competitive-binding assay with blood-group substances and with blood-group A and B active and other oligosaccharides. Carbohydr. Res. *67*, 243–255.

LaTemple, D.C., and Galili, U. (1998). Adult and neonatal anti-Gal response in knock-out mice for alpha1,3galactosyltransferase. Xenotransplantation *5*, 191–196.

Matsuzawa, T., and Ikarashi, Y. (1979). Haemolysis of various mammalian erythrocytes in sodium chloride, glucose and phosphate-buffer solutions. Lab. Anim. *13*, 329–331.

Oblinger, J.L., and Koburger, J.A. (1975). Understanding and teaching the most probable number technique. J. Milk Food Technol. *38*, 540–545.

Ono, T., Tadakuma, T., and Rodriguez, A. (2007). Plasmodium yoelii yoelii 17XNL constitutively expressing GFP throughout the life cycle. Exp. Parasitol. *115*, 310–313.

Platteau, B., Ritz, M., Cormont, F., Wauters, D., and Bazin, H. (1990). Production and Characterization of Rat-Rat Hybridomas against the DNP Hapten (Boca Raton, FL: CRC Press).

Shinkel, T.A., Chen, C.G., Salvaris, E., Henion, T.R., Barlow, H., Galili, U., Pearse, M.J., and d'Apice, A.J. (1997). Changes in cell surface glycosylation in alpha1,3-galactosyltransferase knockout and alpha1,2-fucosyltransferase transgenic mice. Transplantation *64*, 197–204.

Spalter, S.H., Kaveri, S.V., Bonnin, E., Mani, J.C., Cartron, J.P., and Kazatchkine, M.D. (1999). Normal human serum contains natural antibodies reactive with autologous ABO blood group antigens. Blood *93*, 4418–4424.

Tepper, R.I., Coffman, R.L., and Leder, P. (1992). An eosinophil-dependent mechanism for the antitumor effect of interleukin-4. Science *257*, 548–551.

Tran, T.M., Li, S., Doumbo, S., Doumtabe, D., Huang, C.Y., Dia, S., Bathily, A., Sangala, J., Kone, Y., Traore, A., et al. (2013). An intensive longitudinal cohort study of Malian children and adults reveals no evidence of acquired immunity to Plasmodium falciparum infection. Clin. Infect. Dis. *57*, 40–47.

Tsiganov, E.N., Verbina, E.M., Radaeva, T.V., Sosunov, V.V., Kosmiadi, G.A., Nikitina, I.Y., and Lyadova, I.V. (2014). Gr-1dimCD11b+ immature myeloid-derived suppressor cells but not neutrophils are markers of lethal tuberculosis infection in mice. J. Immunol. *192*, 4718–4727.

Walliker, D., Quakyi, I.A., Wellems, T.E., McCutchan, T.F., Szarfman, A., London, W.T., Corcoran, L.M., Burkot, T.R., and Carter, R. (1987). Genetic analysis of the human malaria parasite Plasmodium falciparum. Science *236*, 1661–1666.

Yoshida, N., Nussenzweig, R.S., Potocnjak, P., Nussenzweig, V., and Aikawa, M. (1980). Hybridoma produces protective antibodies directed against the sporozoite stage of malaria parasite. Science *207*, 71–73.
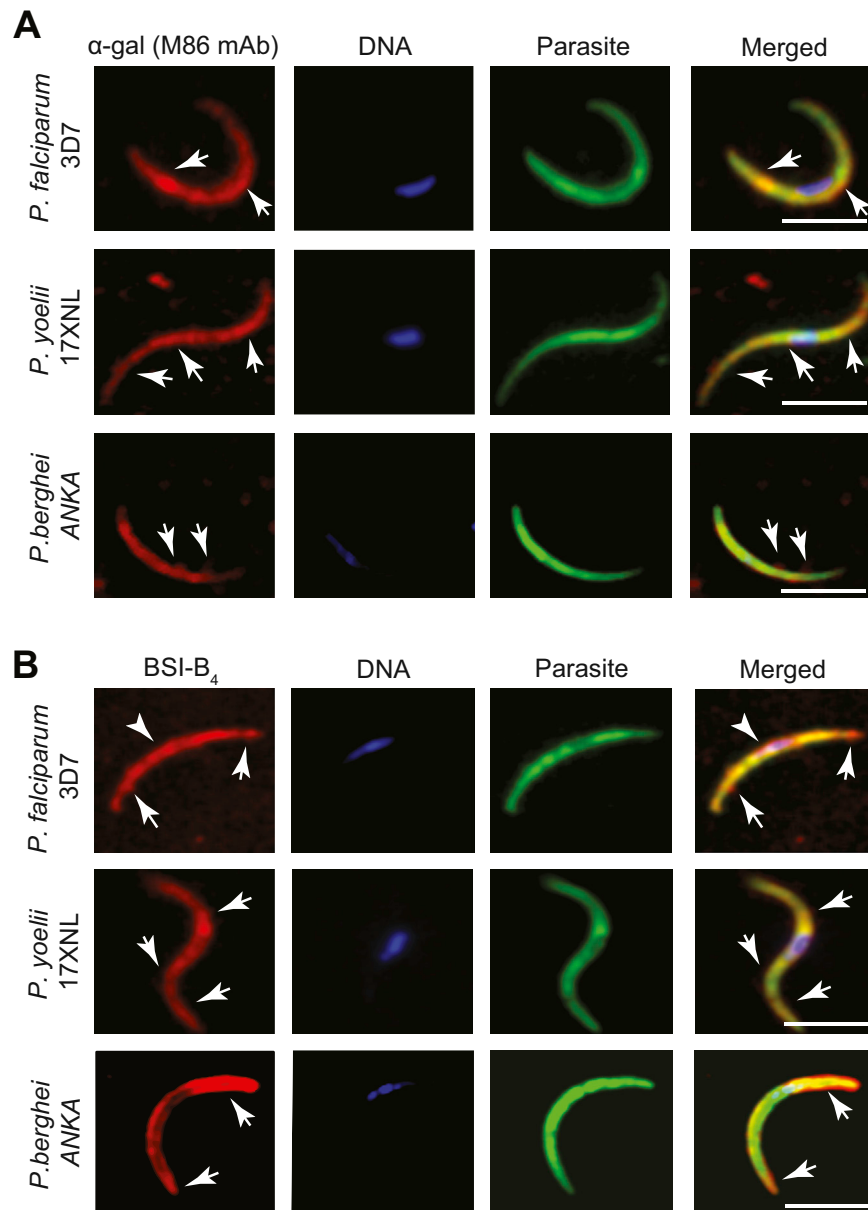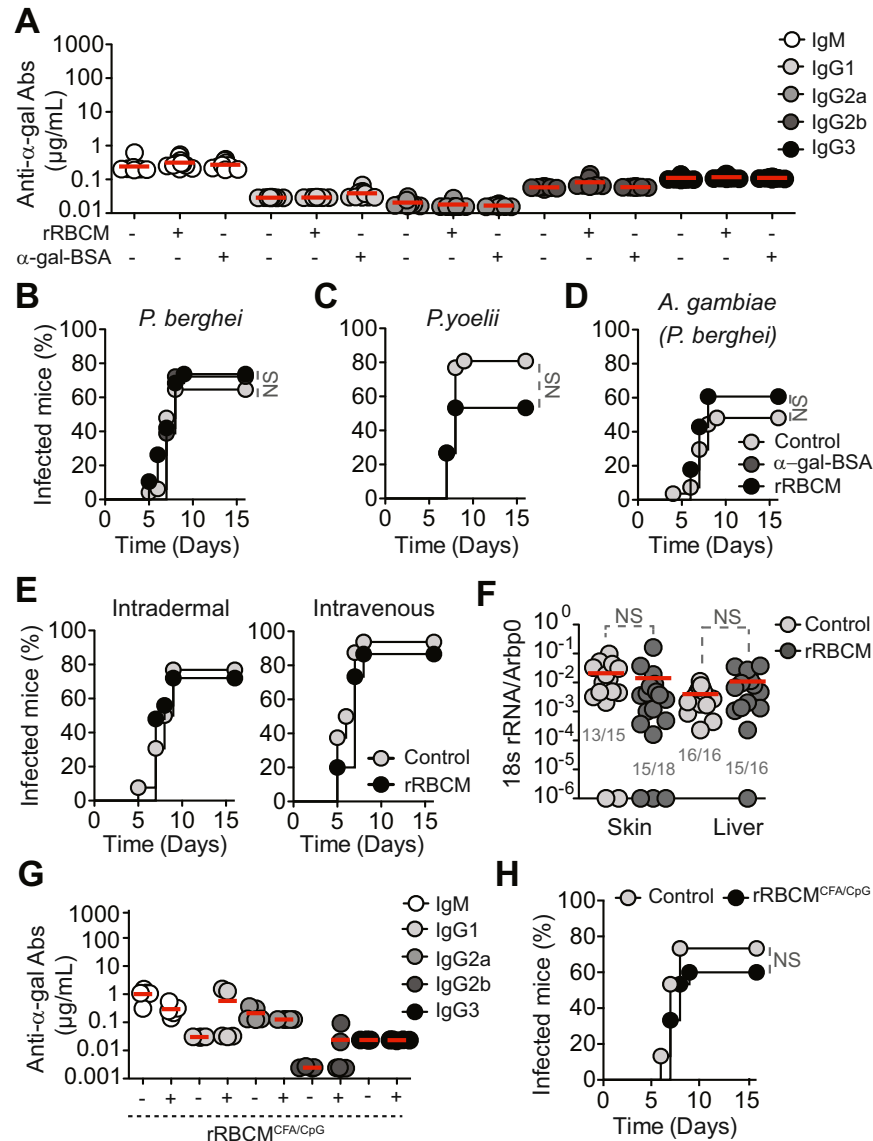
Figure S1. Detection of α-Gal in *Plasmodium* Sporozoites, Related to Figure 1

(A and B) Expression of GFP (*P. berghei* ANKA) and actin (*P. falciparum* 3D7 and *P. yoelli* 17XNL) shown in green, α-gal shown in red and DNA (DAPI) shown in blue. The α-gal epitope was detected with (A) anti-α-gal mAb (M86) or (B) the BSI-B$_4$ lectin. Representative of 2-3 experiments. Arrows indicate α-gal staining. Scale bar, 5 μm.

Figure S2. Anti-α-Gal IgG Abs in Gut-Colonized α1,3Gt$^{−/−}$ Mice and Disease Assessment after Exposure to Infected Mosquitoes, Related to Figure 3

(A) Anti-α-gal IgG subclass Ab levels in α1,3Gt$^{−/−}$ mice not-colonized (SPF), colonized with E. coli K12 or O86.B7 strains after streptomycin treatment (2-3 experiments; n = 12).

(B) Parasitemia (%) and survival (%) in same mice as (A) after exposure to PbA$^{EEF1a-GFP}$ infected A. stephensi mosquitoes (4 experiments; n = 17-34).

(C) Anti-α-gal IgG subclass Ab levels in GF α1,3Gt$^{−/−}$ mice not colonized (GF), colonized with E. coli K12 or O86.B7 strains (2-4 experiments; n = 12).

(D) Parasitemia (%) and survival (%) in same mice as (C) after exposure to PbA$^{EEF1a-GFP}$ infected A. stephensi mosquitoes (4 experiments; n = 7-10 per group).

Mean (red bars).

Figure S3. α1,3Gt^{+/+} Mice Are Not Protected against Malaria Transmission, Related to Figure 4

(A) Anti-α-gal antibodies in the serum of control (-) versus rRBCM (+) or α-gal-BSA (+) immunized α1,3Gt^{+/+} mice (2-3 experiments; n = 12-16).
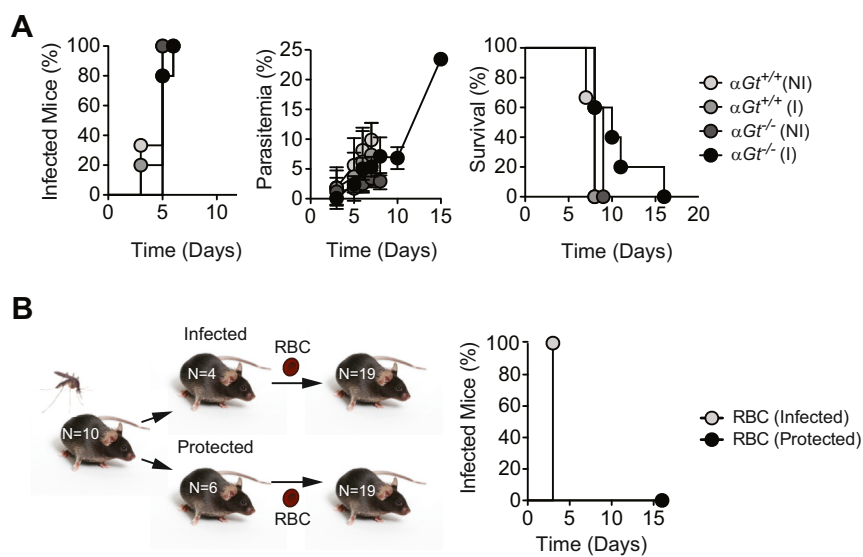
(B–D) Incidence of blood stage of infection (%) in α1,3Gt^{+/+} mice treated as in (A) and exposed to (B) PbA[EEF1a-GFP] infected A. stephensi mosquitoes (7 experiments; n = 19-48), (C) P. yoelii 17XNL infected A. stephensi mosquitoes (5 experiments; n = 26-30) or (D) PbA[EEF1a-GFP] infected A. gambiae mosquitoes (4 experiments; n = 27-28).

(E) Incidence of blood stage of infection (%) in nonimmunized (Control) versus immunized (rRBCM) α1,3Gt^{+/+} mice receiving PbA[EEF1a-GFP] sporozoites (3-4 experiments; n = 15-26).

(F) Plasmodium 18 s rRNA/Arbp0 mRNA in skin and liver of nonimmunized (Control) versus immunized (rRBCM) α1,3Gt^{+/+} mice exposed to PbA[EEF1a-GFP] infected Anopheles stephensi mosquitoes (3-5 experiments). Infected/total mice (gray Nbrs).

(G) Same as (A) in control (-) versus immunized (+; rRBCM emulsified in CFA plus CpG) α1,3Gt^{+/+} mice (2 experiments; n = 5).

(H) Same as (B) in mice treated as in (G) (3 experiments; n = 15). In (A, F and G) dots are individual mice and mean (red bars).

Figure S4. Immunization against α-Gal Is Ineffective in Protecting against Blood Stage of Infection but Confers Sterile Protection against Malaria Transmission, Related to Figure 4

(A) Incidence of blood stage of infection (%; left panel), parasitemia (%; middle panel) and survival (%; right panel) upon inoculation of $PbA^{EEF1a-GFP}$ infected RBC. Mice were either immunized (I) with rRBCM or not immunized (NI) (One experiment; n = 3-5).

(B) Schematic representation of infection protocol (left panel) and incidence of blood stage of infection (%; right panel) in $\alpha 1,3Gt^{-/-}$ mice transferred with RBC from $\alpha 1,3Gt^{-/-}$ mice infected $PbA^{EEF1a-GFP}$ or protected from transmission of $PbA^{EEF1a-GFP}$ infection by *A. stephensi* mosquitoes (2 experiments; n = 19).
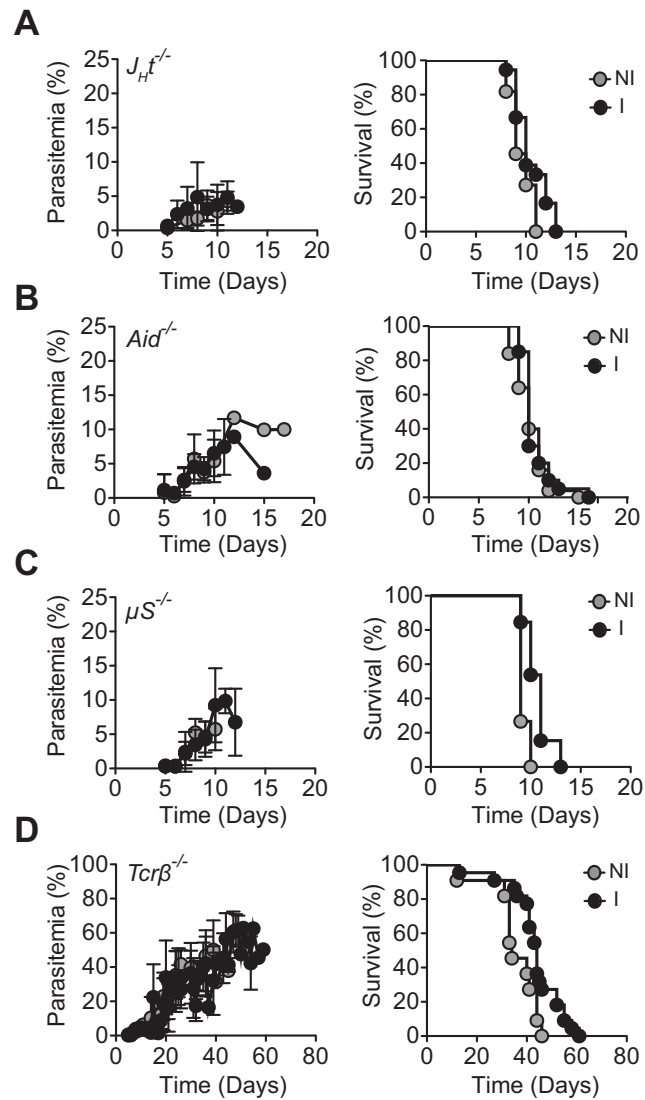
**Figure S5. Blood Stage Infection and Lethality, Related to Figure 5**

(A–D) Parasitemia (%; left panels) and survival (%; right panels) are shown for infected (A) $\alpha 1,3Gt^{-/-}Jht^{-/-}$, (B) $\alpha 1,3Gt^{-/-}Aid^{-/-}$, (C) $\alpha 1,3Gt^{-/-}\mu S^{-/-}$ and (D) $\alpha 1,3Gt^{-/-}Tcr\beta^{-/-}$ mice immunized with rRBCM (I) *vs.* control nonimmunized (NI) (3-7 experiment; n = 11-22).
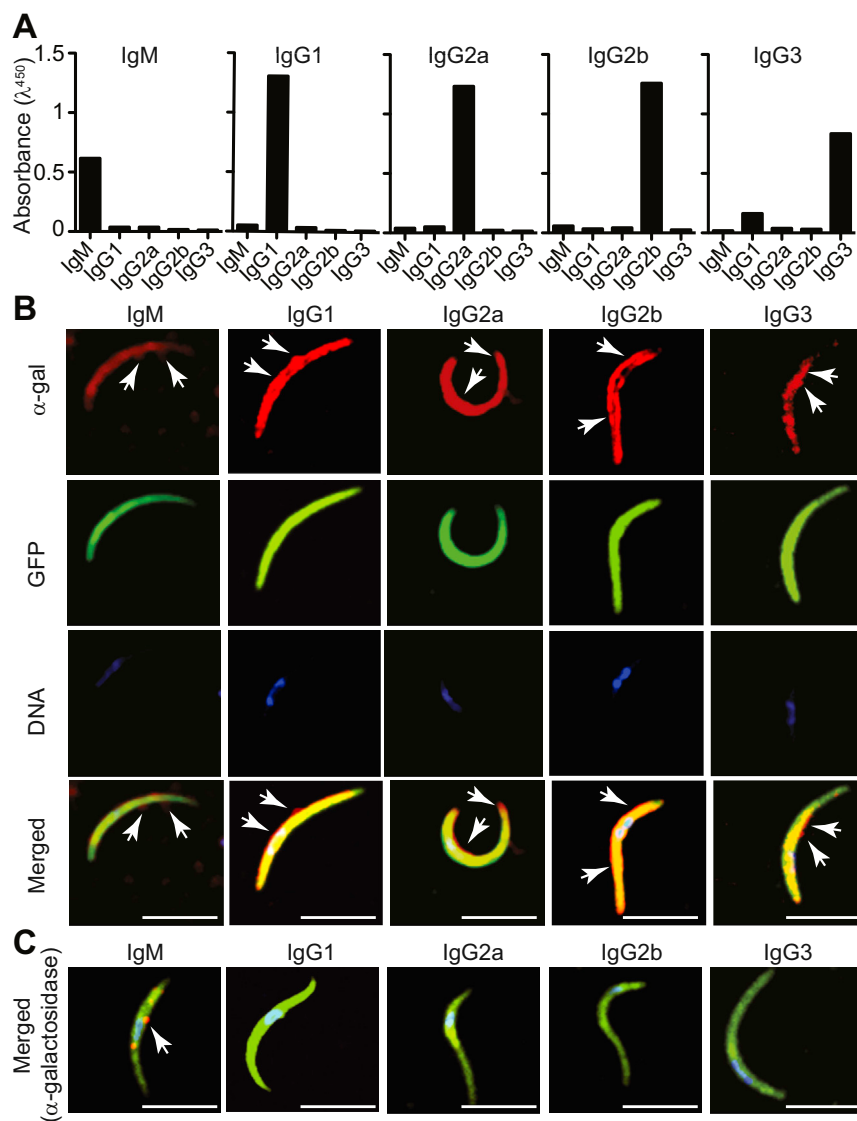
Figure S6. Specificity of Anti-α-Gal mAbs, Related to Figure 5

(A) Comparison of relative binding of anti-α-gal mAbs (125 ng/ml of mAb) determined by ELISA using α-gal-BSA as a solid phase antigen.

(B) Comparison of relative binding capacity of anti-α-gal mAbs (50 μg/ml of mAb) determined by immunofluorescence using *Pb*A$^{EEF1a-GFP}$ sporozoites as an antigen. mAb (red), GFP (green) and DNA (blue) staining. Merged images show composite of the three staining. Representative of 2-3 experiments.

(C) Similar staining as in (*B*) for *Pb*A$^{EEF1a-GFP}$ sporozoites treated with α-galactosidase. Composite images are shown with mAb (red), GFP (green) and DNA (blue) staining. White arrows in (B) and (C) indicate binding of different mAb to the α-gal epitope. Scale bar, 5 μm.
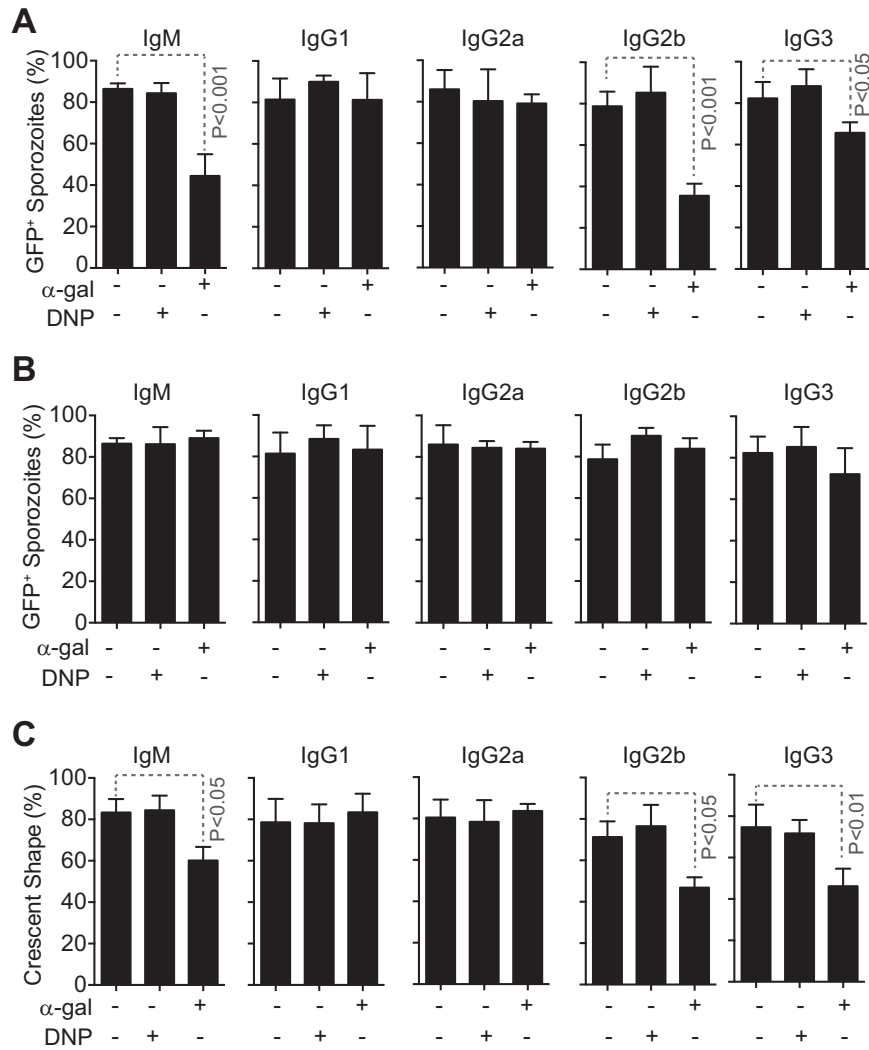
Figure S7. Cytotoxic Effect of Anti-α-Gal Antibodies, Related to Figure 7

(A) Mean percentage (%) of viable GFP$^+$ *Pb*A$^{Hsp70-GFP}$ sporozoites ± STD (3-4 experiments) after in vitro exposure to anti-α-gal (α-gal) or anti-DNP mAbs in the presence of rabbit complement.

(B) Mean percentage (%) of viable GFP$^+$ *Pb*A$^{Hsp70-GFP}$ sporozoites ± STD (3-4 experiments) after in vitro exposure to anti-α-gal (α-gal) or anti-DNP mAbs in the absence of complement.

(C) Mean percentage (%) of viable crescent shaped *Pb*A$^{EEF1a-GFP}$ sporozoites ± STD (3 experiments) after in vitro exposure to anti-α-gal (α-gal) or anti-DNP (DNP) mAb in the presence of mouse complement.